

ANALYSIS OF FOUNDATIONS AND RETAINING WALLS ON INDUSTRIAL WASTE

Vishal Poddar
Pratap Kumar Bebarta



Department of Civil Engineering,
National Institute of Technology Rourkela,
Rourkela – 769008, India

ANALYSIS OF FOUNDATIONS AND RETAINING WALLS ON INDUSTRIAL WASTE

Project Report Submitted in partial fulfillment of the requirements for the degree of

Bachelor of Technology

in

Civil Engineering

by

**Vishal Poddar (107CE007)
Pratap Kumar Bebarta (107CE039)**

Under the guidance of

Prof. S.K. Das



National Institute of Technology Rourkela,
Rourkela – 769008, India.



Department of Civil Engineering
National Institute of Technology Rourkela
Rourkela – 769008, India www.nitrkl.ac.in

CERTIFICATE

This is to certify that the project entitled ***Analysis of Foundations and Retaining Walls on Industrial Waste*** submitted by Mr. ***Vishal Poddar*** (Roll No. **107CE007**) and Mr. ***Pratap Kumar Bebartta*** (Roll. No. **107CE039**) in partial fulfillment of the requirements for the award of Bachelor of Technology Degree in Civil Engineering at NIT Rourkela is an authentic work carried out by them under my supervision and guidance.

Date: 12-5-2011

Prof. S.K. Das
Associate Professor
Department of Civil Engineering
National Institute of Technology Rourkela

ACKNOWLEDGEMENT

We would like to thank **NIT Rourkela** for giving us the opportunity to use their resources and work in such a challenging environment.

First and foremost we take this opportunity to express our deepest sense of gratitude to our guide **Prof. S.K. Das** for his able guidance during our project work. This project would not have been possible without his help and the valuable time that he has given us amidst his busy schedule.

We would also like to extend our gratitude to **Prof. M. Panda**, *Head, Department of Civil Engineering*, who has always encouraged and supported doing our work.

We are also thankful to Mr. P.K. Muduli and Mr. P. Subramaniam, Research Scholar, Geotechnical Engineering and staff members of the **Geotechnical Engineering Laboratory**, for helping and guiding us during the experiments.

Last but not the least we would like to thank all the staff members of Department of Civil Engineering who have been very cooperative with us.

*Vishal Poddar
Pratap Kumar Bebart*

Table of Contents

List of Figures

List of Tables

Abstract	1
Chapter 1	
1.1 Introduction	2
Chapter 2	
2.1 Materials	7
2.2 Laboratory Investigation	11
2.3 Test Results	14
Chapter 3	
3.1 Method of Analysis	26
3.2 Retaining Wall	38
3.3 Inclined Retaining Wall	45
Chapter 4	
4.1 Reliability	47
4.2 Reliability Analysis	48
4.3 Methods of Reliability	50
4.4 Calculation of Reliability Index	52
Chapter 5	
5.1 Conclusion	56
5.2 Scope for future work	57
References	

List of Figures:

Fig. 1.1 Flowchart of Foundation system

Fig. 1.2 Footing in Granular soil or clayey soil

Fig. 1.3 Permissible values of settlement for different types of structures

Fig. 2.1 Typical Figure of Fly ash

Fig. 2.2 Typical Figure of Red mud

Fig. 2.3 Typical Figure of Crusher dust

Fig. 2.4 Typical Figure of Slag

Fig. 2.5 Typical Figure of Proctor test

Fig. 2.6 Water content Density relationship of Sand

Fig. 2.7 Water content Density relationship of Fly ash

Fig. 2.8 Water content Density relationship of Red mud

Fig. 2.9 Water content Density relationship of Crusher dust

Fig. 2.10 Water content Density relationship of Slag

Fig. 2.11 Direct shear test for Sand

Fig. 2.12 Direct shear test for Fly ash

Fig. 2.13 Direct shear test for Red mud

Fig. 2.14 Direct shear test for Crusher dust

Fig. 2.15 Direct shear test for Slag

Fig. 3.1 Typical case of footing on hilly terrain

Fig. 3.2 Schematic diagram of field problem

Fig. 3.3 Geometry of inclined ground with embedded footing

Fig. 3.4 Geometry of embedded footing for angle of inclination of 15°

Fig. 3.5 Settlement of soil for Case-1 (static load)

Fig. 3.6 Force Vs Displacement graph for Case-1 (static load)

Fig. 3.7 Geometry of embedded footing for angle of inclination of 30°

Fig. 3.8 Settlement of soil for Case-2 (static load)

Fig. 3.9 Force Vs Displacement graph for Case-2 (static load)

Fig. 3.10 Geometry of embedded footing for angle of inclination of 60°

Fig. 3.11 Settlement of soil for Case-3 (static load)

Fig. 3.12 Force Vs Displacement graph for Case-3 (static load)

Fig. 3.13 Force Vs Displacement graph for Case-1 (seismic load)

Fig. 3.14 Force Vs Displacement graph for Case-2 (seismic load)

Fig. 3.15 Force Vs Displacement graph for Case-3 (seismic load)

Fig. 3.16 Force Vs Displacement graph for Case-4 (seismic load)

Fig. 3.17 Force Vs Displacement graph for Case-5 (seismic load)

Fig. 3.18 Force Vs Displacement graph for Case-6 (seismic load)

Fig. 3.19 Schematic diagram of Retaining wall

Fig 3.20 Deformed mesh of retaining wall for sand

Fig 3.21 Distribution of effective stress on retaining wall by sand

Fig 3.22 Deformed mesh of retaining wall for fly ash

Fig 3.23 Distribution of effective stress on retaining wall by fly ash

Fig 3.24 Deformed mesh of retaining wall for red mud

Fig 3.25 Distribution of effective stress on retaining wall by red mud

Fig 3.26 Deformed mesh of retaining wall for crusher dust

Fig 3.27 Distribution of effective stress on retaining wall by crusher dust

Fig 3.28 Deformed mesh of retaining wall for crusher dust

Fig 3.29 Distribution of effective stress on retaining wall by slag

Fig 3.30 Active earth pressure against angle of inclination of wall for different materials

Fig. 4.1 The overlapped area as probability of failure of random variable R and L

Fig. 4.2 Distribution of safety margin, $Z = R-L$ (*Melchers 2002*)

Fig. 4.3 Bearing capacity of individual industrial waste

Fig. 4.4 Bearing capacity of combined industrial waste (using Terzaghi's equation)

Fig. 4.5 Bearing capacity of combined industrial waste (using equation 4.11)

Fig. 4.6 Reliability Index for the combination of sample

List of Tables:

Table 1.1 The bearing capacity factors

Table 2.1 Specific Gravity of Sand

Table 2.2 Specific Gravity of Fly ash

Table 2.3 Specific Gravity of Red Mud

Table 2.4 Specific Gravity of crusher dust

Table 2.5 Specific Gravity of slag

Table 2.6 Specific Gravity of all samples

Table 2.7 Table Vibrator Test

Table 2.8 MDD as per different tests; Vibratory, Standard, Modified Proctor test

Table 2.9 Cohesion, Angle of friction for different materials

Table 4.1 The expected levels of Performance in terms p_f and corresponding β

(U.S. Army Corps of Engineers 1999)

ABSTRACT

The accumulation of industrial waste has poses a serious problem to the industrial growth and to human habitation. Disposal of industrial waste is covering vast track of valuable land. In this study an attempt has been made to evaluate the properties of industrial wastes like fly ash, red mud, crusher dust, blast furnace slag to use as foundation bed and backfill in retaining structures. As most of the industrials wastes are dumped as heaps, studies have been carried out for the footings embedded in sloping ground. Various research have been done in the seismic bearing capacity of footings for horizontal ground, but the study for sloping ground is very limited. The effect of seismic forces on the above footings is also studied using finite element method. The inclined retaining walls with industrial wastes as backfill was analysed. As the variation in geotechnical properties of industrial wastes are obvious due to various reasons, lastly, reliability analysis of foundations on industrial waste using tradition limit equilibrium method is also studied, considering the variability of the parameters contributing to the performance of the system.

CHAPTER-1

INTRODUCTION

1.1. INTRODUCTION

Foundation is that part of the structure which transmits the load from the superstructure to the soil without any kind of distress in the superstructure as well as the soil. The foundation also known as substructure can be broadly classified into two types; (i) Foundation structure and (ii) Retaining structure. The foundation structure is mainly subjected to vertical loads, transmitted from the super structure while the retaining structure is mainly subjected to the horizontal loads, the earth pressures. As both the structures are concerned with the contact with the soil, so it has been classified under the Foundation Systems as the broader field.

The figure below shows the flowchart of the foundation system showing the foundation structure and retaining structure outlay

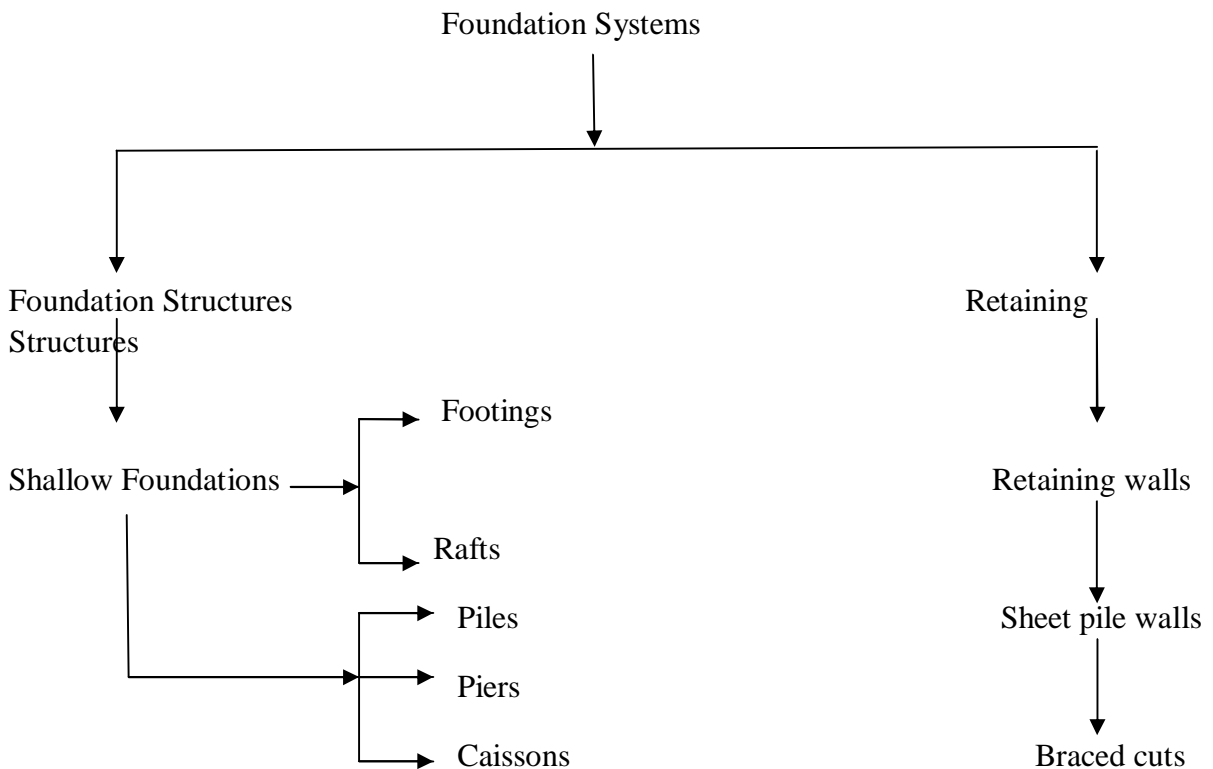


Fig. 1.1 Flowchart of Foundation system

Estimation of bearing capacity of foundation is an important parameter in the design of any substructures. In geotechnical engineering, ***bearing capacity*** is the capacity of soil to support the loads applied to the ground. The bearing capacity of soil is the maximum average contact pressure between the foundation and the soil which should not produce shear failure in the soil. ***Ultimate bearing capacity*** is the theoretical maximum pressure which can be supported without failure; ***allowable bearing capacity*** is the ultimate bearing capacity divided by a factor of safety. Sometimes, on soft soil sites, large settlements may occur under loaded foundations without actual shear failure occurring; in such cases, the allowable bearing capacity is based on the maximum allowable settlement.

Structures such as retaining walls, transmission towers and bridge abutments often involve the construction of footings on sloping ground. Construction of footings below inclined ground is also a common practice because of land cost effectiveness or to maintain natural terrain of the ground or for many other reasons. Limited studies have been carried out for the footings embedded in sloping ground (Meyerhof (1957, 1963), Hansen (1970), Vesic (1973)). Research in seismic bearing capacity is in much demand due to the devastating effect of the foundations under earthquake conditions. Various research have been done in the seismic bearing capacity of footings for horizontal ground, but the study for sloping ground is very limited. And also most of the literatures are concerned with the evaluation of the bearing capacity of foundations on slopes for the static condition but very limited information is available to predict the response of foundations on inclined ground during an earthquake. This study also deals with the industrial waste as an alternate geotechnical engineering material instead of natural soil. Brief introduction about the bearing capacity particularly on the sloping ground, retaining wall and the industrial wastes used in the present study is presented as follows. The results are also compared with footing and retaining wall with sand.

TERZAGHI'S EQUATIONS FOR BEARING CAPACITY (IS: 6403-1981)

a) In case of general shear failure $q_f = cN_c S_c i_c d_c + q(N_q - 1)S_q i_q d_q + 0.5\gamma B N_\gamma S_\gamma i_\gamma d_\gamma W'$ (1.1a)

b) In case of local shear failure $q_f = cN'_c S_c i_c d_c + q(N'_q - 1)S_q i_q d_q + 0.5\gamma B N'_\gamma S_\gamma i_\gamma d_\gamma W'$ (1.1b)

SHAPE FACTORS

Shape	Strip	Circle	Square	Rectangle
S_c	1.0	1.3	1.3	$1 + 0.2 B/L$
S_q	1.0	1.2	1.2	$1 + 0.2 B/L$
S_γ	1.0	0.6	0.8	$1 - 0.4 B/L$

DEPTH FACTORS

$$d_c = 1 + 0.2D_f/B\sqrt{N\phi} \quad (1.2)$$

$$d_q = d_\gamma = 1 \text{ for } \phi < 10^\circ \quad (1.3a)$$

$$d_q = d_\gamma = 1 + 0.1D_f/B\sqrt{N\phi} \text{ for } \phi > 10^\circ \quad (1.3b)$$

INCLINATION FACTORS

$$i_c = i_q = \left(1 - \frac{\alpha}{90}\right)^2 \quad (1.4)$$

$$i_\gamma = \left(1 - \frac{\alpha}{90}\right)^2 \quad (1.5)$$

Effect of water table

- If the water table is likely to permanently remain at or below a depth of $(D_f + B)$ beneath the ground level surrounding the footing then $W' = 1$.
- If the water table is located at a depth D_f or likely to rise to the base of the footing or above then the value of W' shall be taken as 0.5.

c) If the water table is likely to permanently get located at depth $D_f < D_w < (D_f + B)$, then the value of W' be obtained by linear interpolation.

BEARING CAPACITY FACTORS

Table 1.1 – Shows the bearing capacity factors

ϕ (Degrees)	N_c	N_q	N_γ
0	5.14	1.00	0.00
5	6.49	1.57	0.45
10	8.35	2.47	1.22
15	1.98	3.94	2.65
20	14.83	6.40	5.39
25	20.72	10.66	10.88
30	30.14	18.40	22.40
35	46.12	33.30	48.03
40	75.31	64.20	19.41
45	138.88	134.88	271.76
50	266.89	319.07	762.89

Note – For obtaining N_c' , N_q' , N_γ' corresponding to local shear failure, calculate

$\phi' = \tan^{-1}(0.67\phi)$. Read N_c , N_q , N_γ from above table corresponding to the value of ϕ' instead of ϕ which are the values of N_c' , N_q' , N_γ' respectively.

IS Code 1904-1986

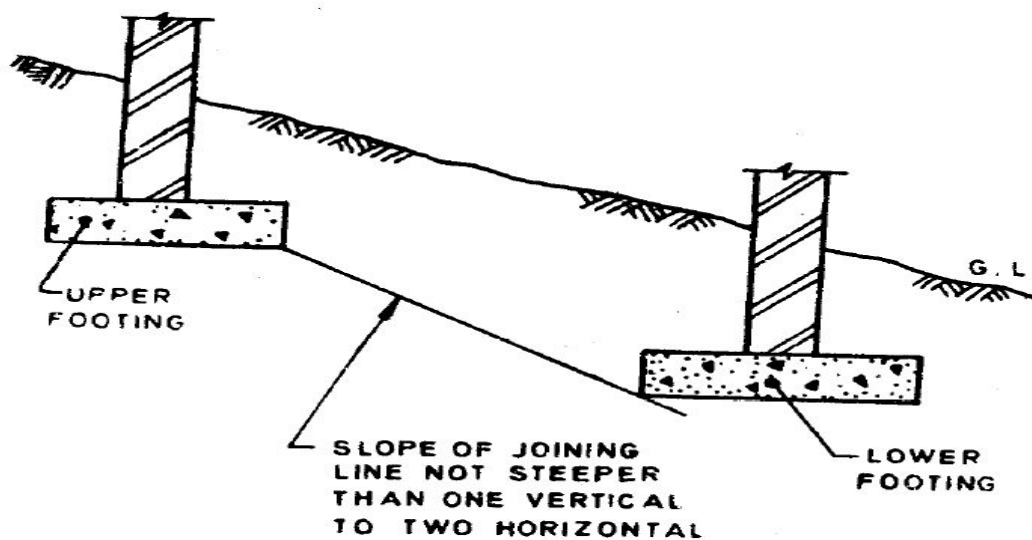


Fig. 1.2 Footing in Granular soil or clayey soil

Criteria for Settlement Analysis for Shallow Foundation

Sl No.	Type of Structure	ISOLATED FOUNDATIONS						RAFT FOUNDATIONS					
		Sand and Hard Clay			Plastic Clay			Sand and Hard Clay			Plastic Clay		
		Maximum settlement	Differential settlement	Angular distortion	Maximum settlement	Differential settlement	Angular distortion	Maximum settlement	Differential settlement	Angular distortion	Maximum settlement	Differential settlement	Angular distortion
		mm	mm	mm	mm	mm	mm	mm	mm	mm	mm	mm	mm
(1)	(2)	(3)	(4)	(5)	(6)	(7)	(8)	(9)	(10)	(11)	(12)	(13)	(14)
	i) For steel structure	50	0.0033L	1/300	50	0.0033L	1/300	75	0.0033L	1/300	100	0.0033L	1/300
	ii) For reinforced concrete structures	50	0.0015L	1/666	75	0.0015L	1/666	75	0.0021L	1/500	100	0.002L	1/500
	iii) For multistoreyed buildings												
	a) RC or steel framed buildings with panel walls	60	0.002L	1/500	75	0.002L	1/500	75	0.0025L	1/400	125	0.0033L	1/300
	b) For load bearing walls												
	1) L/H = 2+	60	0.002L	1/5000	60	0.002L	1/5000	Not likely to be encountered					
	2) L/H = 7+	60	0.004L	1/2500	60	0.004L	1/2500						
	iv) For water towers and silos	50	0.0015L	1/666	75	0.0015L	1/666	100	0.0025L	1/400	125	0.0025L	1/400

NOTE — The values given in the table may be taken only as a guide and the permissible total settlement/different settlement and tilt (angular distortion) in each case should be decided as per requirements of the designer.
L denotes the length of deflected part of wall/raft or centre-to-centre distance between columns.
H denotes the height of wall from foundation footing.
*For intermediate ratios of L/H, the values can be interpolated.

Fig. 1.3 Permissible values of settlement for different types of structures

CHAPTER-2
MATERIALS AND LABORATORY
INVESTIGATIONS

2.1 MATERIALS

The following samples were used and some experiments were conducted on this sample for comparison and knowing about the soil behaviours for different materials. The experiments which were conducted are briefly discussed. The samples were collected from different site and the results concluded form the experiment gives the property of soil for that site only.

FLY ASH

The fly-ash is a fairly divided residue which results from the combustion of ground or powdered bituminous coal or sub-bituminous coal like lignite and transported by the flue gases of boilers fired by pulverized coal or lignite. Fly ash is generally captured by electrostatic precipitators or other particle filtration equipments before the flue gases reach the chimneys of coal-fired power plants, and together with bottom ash removed from the bottom of the furnace is in this case jointly known as coal ash. Depending upon the source and makeup of the coal being burned, the components of fly ash vary considerably, but all fly ash includes substantial amounts of silicon dioxide (SiO_2) (both amorphous and crystalline) and calcium oxide (CaO), both being endemic ingredients in many coal-bearing strata. Fly-ash contains some un-burnt carbon. It is acidic in nature and its main constituents are silica, aluminum oxide and ferrous oxide.



Fig. 2.1 Typical Figure of Fly ash

RED MUD

Red mud is a solid waste product of the Bayer process, the principal industrial means of refining bauxite in order to provide alumina as raw material for the electrolysis of aluminium by the Hall–Héroult process. Red mud is composed of a mixture of solid and metallic oxide-bearing impurities, and presents one of the aluminium industry's most important disposal problems. The red colour is caused by the oxidised iron present, which can make up to 60% of the mass of the red mud. In addition to iron, the other dominant particles include silica, unleached residual aluminium, and titanium oxide. Red mud cannot be disposed of easily. In most countries where red mud is produced, it is pumped into holding ponds. Red mud presents a problem as it takes up land area and can neither be built on nor farmed, even when dry. Due to the Bayer process the mud is highly basic with a pH ranging from 10 to 13. Several methods are used to lower the alkaline pH to an acceptable level to decrease the impact on the environment.



Fig. 2.2 Typical Figure of Red mud

CRUSHER DUST

When furnaces and quarrying procedures produce slag from treating different types of stone, manufacturers gather this slag together and grind it down into crusher dust. This dust is made of a variety of materials, but often contains a large amount of silicates and alumina-silicates. In appearance, crusher dust has a greyish or brownish tone with very fine aggregate particles, like soft sand. These particles, when looked at under a microscope, are rough cubes and individually have a rough surface texture. Crusher dust has many of the useful properties of the stone that it comes from. It is very heat resistant and contains no plastic chemicals that may be toxic to the surrounding environment over time. The chemical nature of crusher dust is very dependable and largely alkaline. So that it can be used in variety of material. It is also durable, strong, and can be easily compressed into tight spaces. Crusher dust is primarily used as filler and cement aggregate. Sometimes it can also be used as the replacement for fine aggregates in the concrete. When used in concrete, the crusher dust mixes in with larger aggregate to help form a specific texture. The dust is also used to make mortar and other similar materials.



Fig. 2.3 Typical Figure of Crusher dust

SLAG

Slag is a partially vitreous by-product of smelting ore to separate the metal fraction from the unwanted fraction. It can usually be considered to be a mixture of metal oxides and silicon dioxide. However, slag can contain metal sulphides and metal atoms in the elemental form. While slag are generally used as a waste removal mechanism in metal smelting, they can also serve other purposes, such as assisting in the temperature control of the smelting; and also minimizing any re-oxidation of the final liquid metal product before the molten metal is removed from the furnace and used to make solid metal. Ferrous and non-ferrous smelting processes produce different slag. The smelting of copper and lead in non-ferrous smelting, for instance, is designed to remove the iron and silica that often occurs with those ores, and separates them as iron-silicate-based slag.



Fig. 2.4 Typical Figure of Slag

2.2 LABORATORY INVESTIGATION

Soil Compaction

Soil compaction is defined as the method of mechanically increasing the density of soil. In construction, this is a significant part of the building process. If performed improperly, settlement of the soil could occur and result in unnecessary maintenance costs or structure failure. Almost all improperly, settlement of the soil could occur and result in unnecessary maintenance costs or structure failure.

These different types of effort in field are found in the two principle types of compaction force: static and vibratory.

1. **Static force** is simply the deadweight of the machine, applying downward force on the soil surface, compressing the soil particles. The only way to change the effective compaction force is by adding or subtracting the weight of the machine. Static compaction is confined to upper soil layers and is limited to any appreciable depth. Kneading and pressure are two examples of static compaction.

2. **Vibratory force** uses a mechanism, usually engine-driven, to create a downward force in addition to the machine's static weight. The vibrating mechanism is usually a rotating eccentric weight or piston/spring combination (in rammers). The compactors deliver a rapid sequence of blows (impacts) to the surface, thereby affecting the top layers as well as deeper layers.

Factors affecting Compaction:

Various factors affecting compactions are: (1) Water content (2) Amount of compaction (3) Method of compaction (4) Type of soil (5) Addition of admixtures

STANDARD PROCTOR COMPACTION TEST:

The proctor test was developed by R.R Proctor in the year 1933 for the construction of earth fill dams in the state of California. The Indian standard IS: 2720 (part VII) was followed in the present study.

MODIFIED PROCTOR TEST:

The modified proctor test was developed to give a higher standard of compaction. In this test the soil is compacted in the standard proctor test mould but in 5 layers instead of as in standard Proctor test. The Indian standard IS: 2720 (part VIII) was followed in the present study.

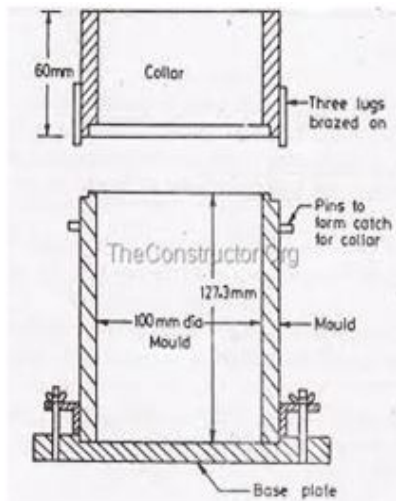


Fig. 2.5 Typical Figure of Proctor test

COMPACTION USING TABLE VIBRATOR:

The samples were compacted in a table vibrator to find out the maximum and minimum void ratio.

SPECIFIC GRAVITY:

This test is done to determine the specific gravity of fine-grained soil by density bottle method as per IS: 2720 (Part III/Sec 1) – 1980. Specific gravity is the ratio of the weight in air of a given volume of a material at a standard temperature to the weight in air of an equal volume of distilled water at the same stated temperature.

REPORTING OF RESULTS

The specific gravity G of the soil = $(W_2 - W_1) / [(W_4 - W_1) - (W_3 - W_2)]$

The specific gravity should be calculated at a temperature of 27°C and reported to the nearest 0.01. If the room temperature is different from 27°C, the following correction should be done:

$$G' = kG \quad (2.1)$$

Where,

G' = Corrected specific gravity at 27°C

k = [Relative density of water at room temperature]/ Relative density of water at 27°C.

DIRECT SHEAR TEST

A direct shear test also known as shearbox test is a laboratory or field test used by geotechnical engineers to measure the shear strength properties of soil or rock materials or of discontinuities in soil or rock masses. IS: 2720 (Part XIII) was followed to establish the shear strength properties of soil.

2.3 TEST RESULTS

1. SPECIFIC GRAVITY

Specific gravity of Sand

Relative density, sometimes called specific mass or specific gravity, is the ratio of the density (mass of a unit volume) of a substance to the density of a given reference material. The specific gravity of the sand is determined using the specific gravity bottle. The average specific gravity of the sand is found to be **2.68**. The results are presented in the Table 2.1.

Table 2.1 Specific Gravity of Sand

Wt. of density bottle (gm)	Density bottle + dry soil wt.(gm)	Density bottle + wet soil wt. (gm)	Density bottle + water wt. (gm)	Specific gravity
109.60	159.60	389.80	358.50	2.67
100.20	150.20	380.50	349.10	2.69
116.49	166.49	396.70	365.28	2.69

Average specific gravity = 2.68

Specific gravity of Fly ash

The average specific gravity of the fly ash is found to be **1.98**. The results are presented in the Table 2.2.

Table 2.2 Specific Gravity of Fly ash

Wt. of density bottle (gm)	Density bottle + dry soil wt.(gm)	Density bottle + wet soil wt.(gm)	Density bottle+ water wt.(gm)	Specific gravity
107.00	157.00	380.40	355.70	1.98
88.34	138.34	311.80	287.05	1.98
117.10	167.10	390.50	365.90	1.97

Average specific gravity = 1.98

Specific gravity of Red mud

The average specific gravity of the red mud is found to be **3.06**. The results are presented in the Table 2.3.

Table 2.3 Specific Gravity of Red Mud

Wt. of density bottle (gm)	Density bottle + dry soil wt.(gm)	Density bottle + wet soil wt.(gm)	Density bottle+ water wt.(gm)	Specific gravity
112.46	162.46	395.00	361.31	3.07
116.25	166.25	398.70	365.10	3.05
124.75	174.75	407.20	373.49	3.07

Average specific gravity = 3.06

Specific gravity of crusher dust

The average specific gravity of the crusher dust is found to be **2.70**. The results are presented in the Table 2.4.

Table 2.4 Specific Gravity of crusher dust

Wt. of density bottle (gm)	Density bottle + dry soil wt.(gm)	Density bottle + wet soil wt.(gm)	Density bottle+ water wt.(gm)	Specific gravity
117.10	167.10	397.40	365.90	2.70
96.49	146.49	326.90	295.50	2.69
88.34	138.34	318.50	287.05	2.70

Average specific gravity = 2.70

Specific gravity of slag

The average specific gravity of the slag is found to be **2.75**. The results are presented in the **Table 2.5**.

Table 2.5 Specific Gravity of slag

Wt. of density bottle (gm)	Density bottle + dry soil wt.(gm)	Density bottle + wet soil wt.(gm)	Density bottle + water wt. (gm)	Specific gravity
114.40	164.40	394.80	363.00	2.75
112.46	162.46	393.20	361.31	2.76
92.36	142.36	373.05	341.20	2.75

Average specific gravity = 2.75

Table 2.6 Specific Gravity of all samples

MATERIALS	SPECIFIC GRAVITY
SAND	2.68
FLY ASH	1.98
RED MUD	3.06
CRUSHER DUST	2.70
SLAG	2.75

From the Table 2.6 it can be seen that the red mud is has the highest specific gravity of 3.06 among all the five industrial waste used, while fly ash has the lowest specific gravity of 1.98. Crusher dust and sand have almost the same specific gravity.

2. PROCTOR TEST

SAND

The compaction curve for sand is presented in Figure 2.7. The optimum moisture content (OMC) is found to be **11.35%** and maximum dry density (MDD) as **1.49 gm/cm³** for standard Proctor test. Similarly the result as per modified Proctor compaction for OMC and MDD is found to be **12.69%** and **1.66 gm/cm³** respectively.

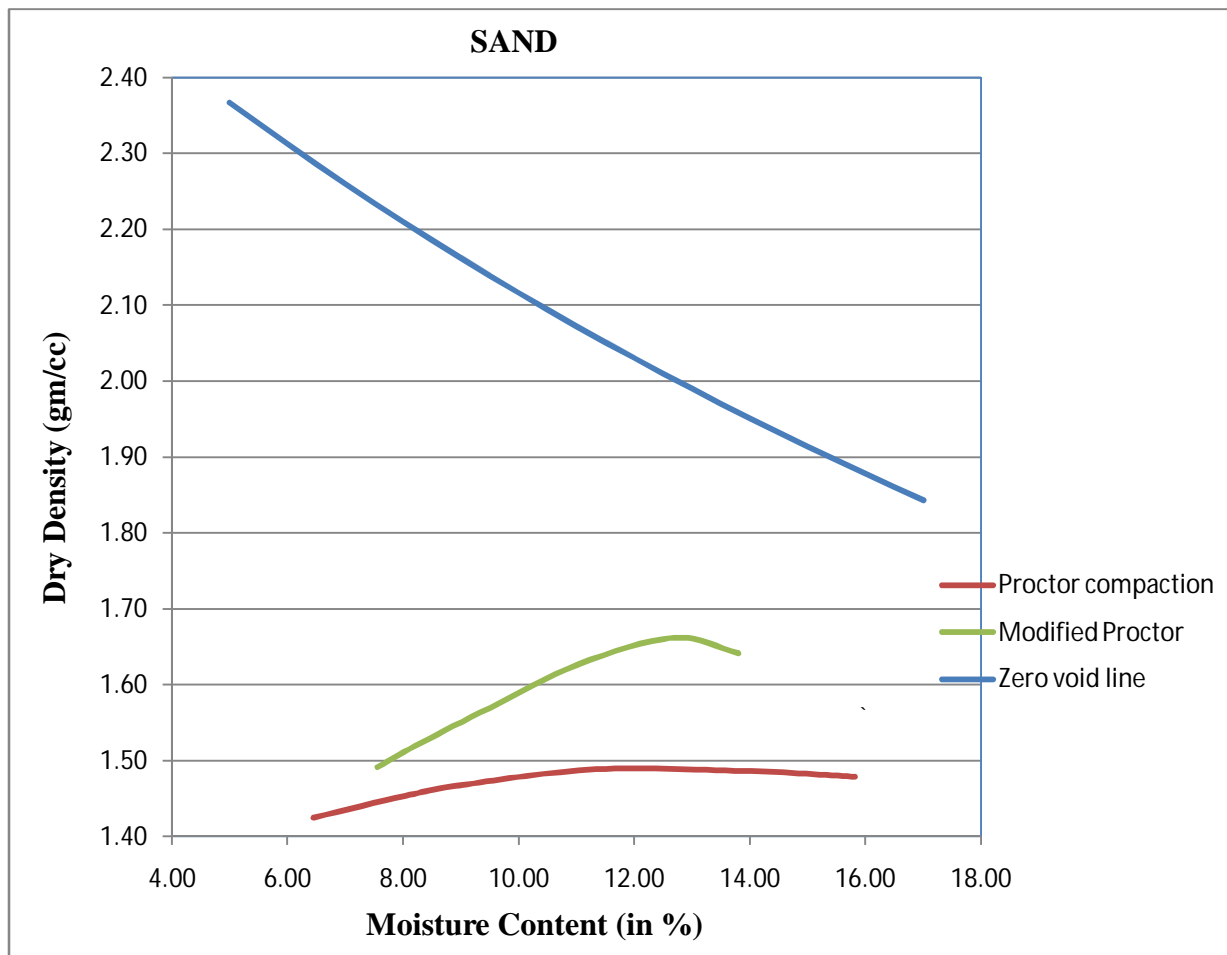


Fig. 2.6 Water content Density relationship of Sand

FLY ASH

The compaction curve for sand is presented in Figure 2.8. The optimum moisture content (OMC) is found to be **19.73%** and maximum dry density (MDD) as **1.29 gm/cm³** for standard Proctor test. Similarly the result as per modified Proctor compaction for OMC and MDD is found to be **11.96%** and **1.40 gm/cm³** respectively.

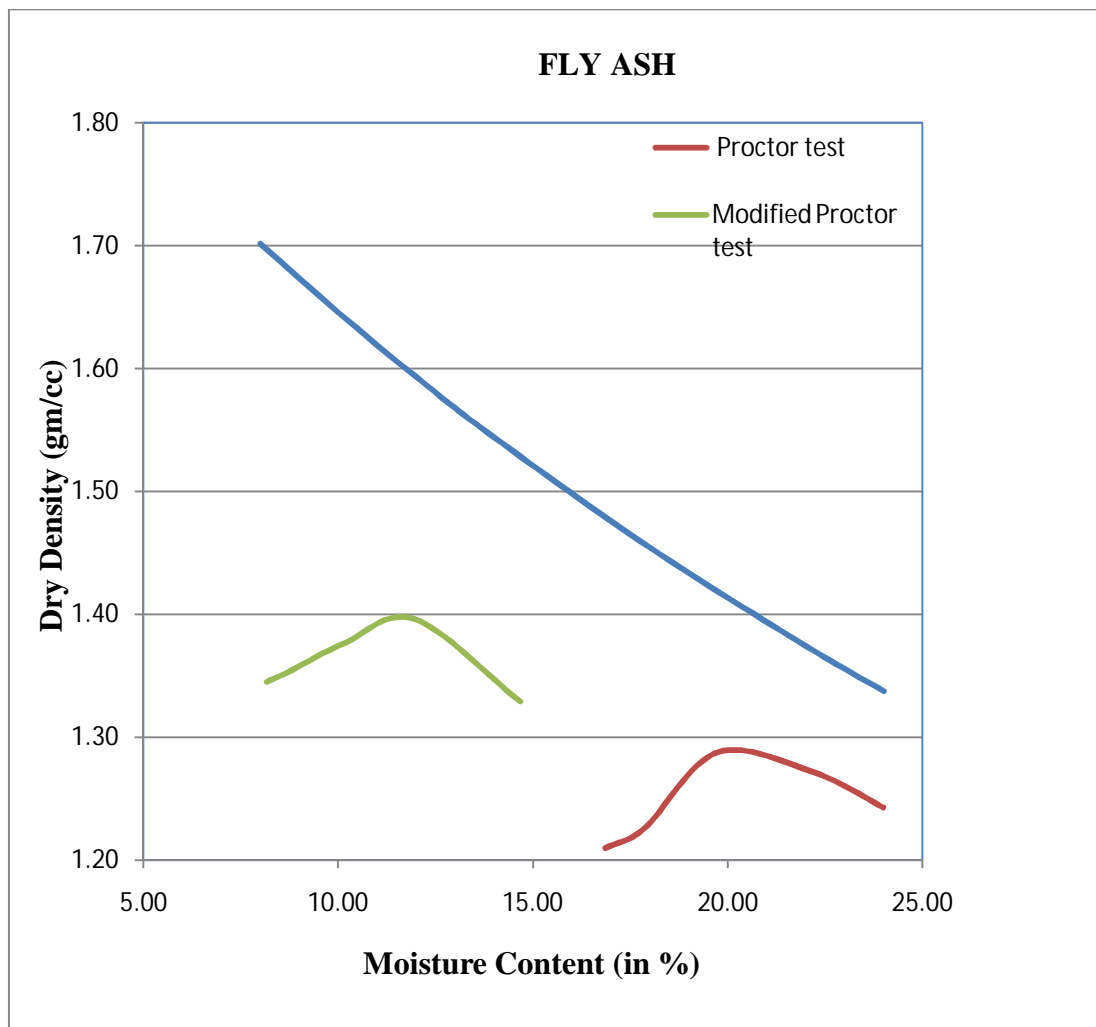


Fig. 2.7 Water content Density relationship of Fly ash

RED MUD

The compaction curve for sand is presented in Figure 2.9. The optimum moisture content (OMC) is found to be **11.46%** and maximum dry density (MDD) as **2.05 gm/cm³** for standard Proctor test. Similarly the result as per modified Proctor compaction for OMC and MDD is found to be **10.91%** and **2.15 gm/cm³** respectively.

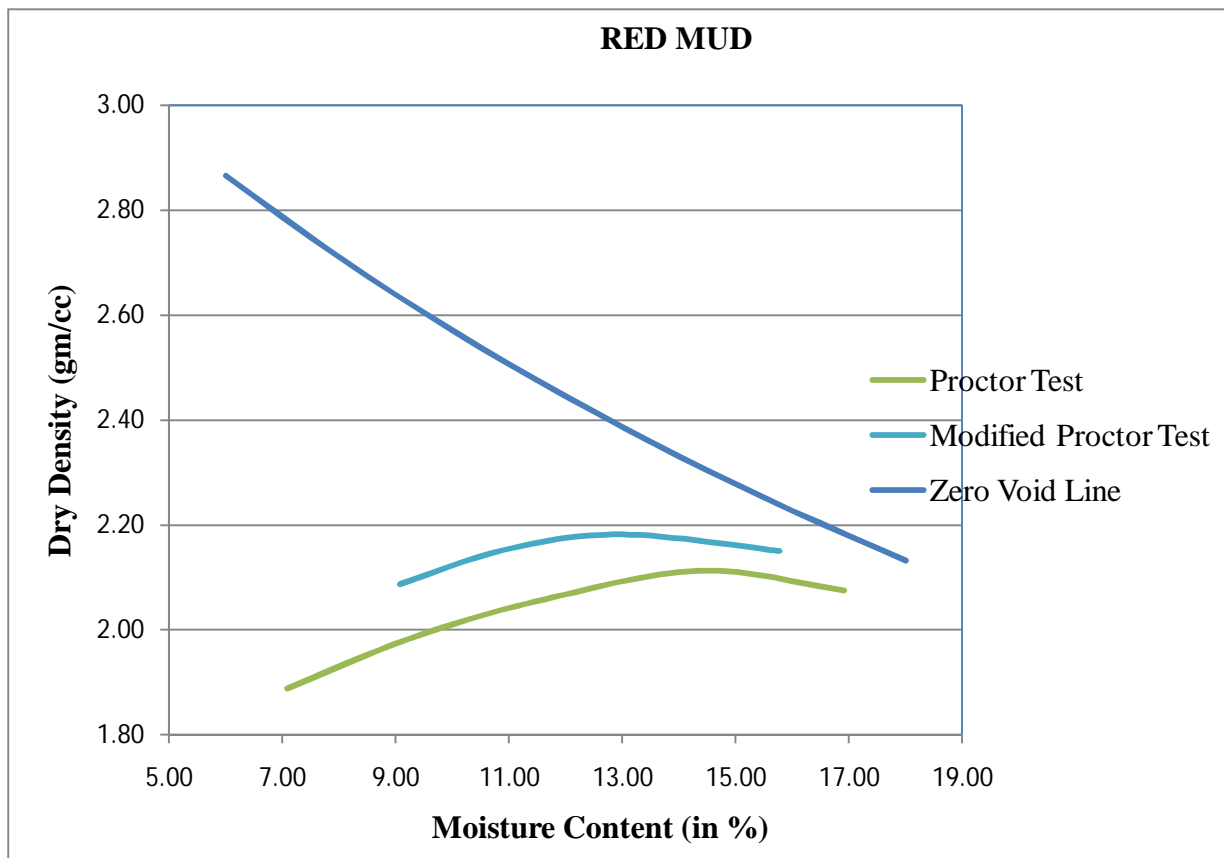


Fig. 2.8 Water content Density relationship of Red mud

CRUSHER DUST

The compaction curve for sand is presented in Figure 2.10. The compaction characteristics were studied using both Standard Proctor and Modified Proctor compaction tests as per Indian Standards. The optimum moisture content (OMC) is found to be **9.43%** and maximum dry density (MDD) as **2.04 gm/cm³** for standard Proctor test. Similarly the result as per modified Proctor compaction for OMC and MDD is found to be **8.62%** and **2.11 gm/cm³** respectively.

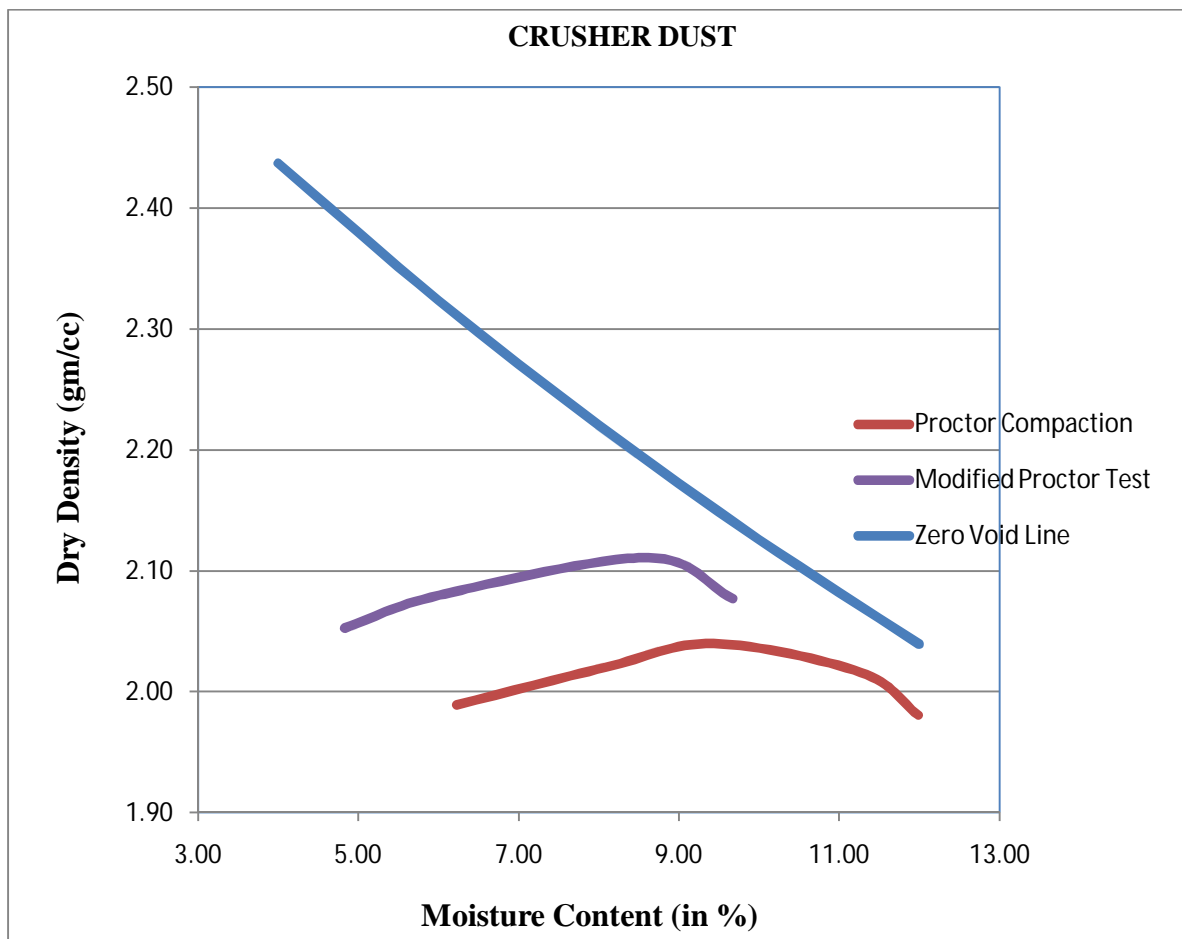


Fig. 2.9 Water content Density relationship of Crusher dust

SLAG

The compaction curve for sand is presented in Figure 2.11. The compaction characteristics were studied using both Standard Proctor and Modified Proctor compaction tests as per Indian Standards. The optimum moisture content (OMC) is found to be **18.15%** and maximum dry density (MDD) as **2.04 gm/cm³** for standard Proctor test. Similarly the result as per modified Proctor compaction for OMC and MDD is found to be **14.68%** and **2.16 gm/cm³** respectively.

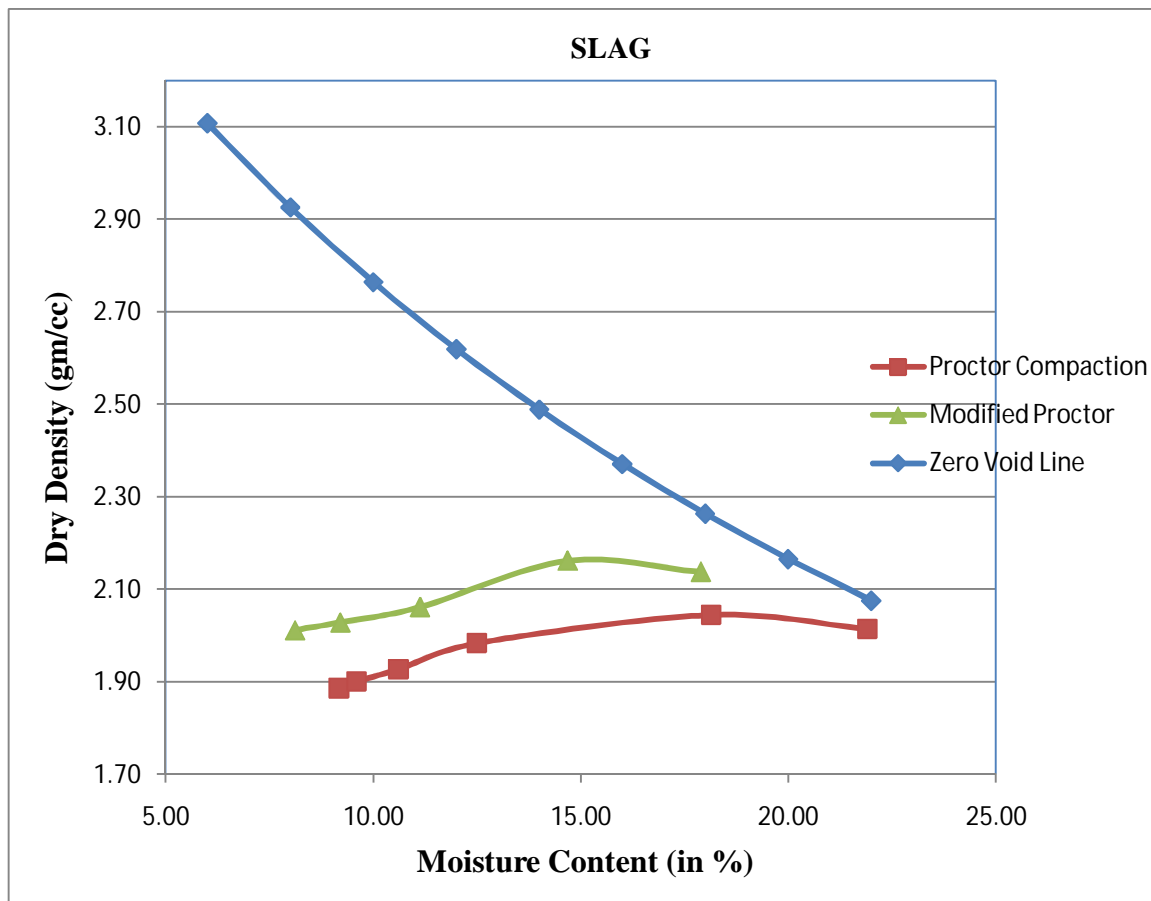


Fig. 2.10 Water content Density relationship of Slag

3. TABLE VIBRATOR TEST

The test data for vibratory table is presented in Table 2.7. It can be seen that red mud shows the highest maximum density among all the industrial waste used. Fly ash has the highest maximum void ratio, while slag has the lowest void ratio.

Table 2.7 Table Vibrator Test

Sample	Weight in loosest state(gm)	Minimum density (gm/cc)	Weight in compacted state(gm)	Maximum density (gm/cc)	Maximum void ratio	Minimum void ratio
Sand	4051	1.34	4563	1.51	1	0.77
Crusher dust	4908	1.63	6091	2.02	0.65	0.34
Slag	5744	1.91	6345	2.05	0.44	0.18
Fly ash	2704	0.90	3534	1.19	1.16	0.80
Red Mud	3120	1.83	3678	2.14	0.67	0.43

Table 2.8 shows the comparative results of maximum dry density for all the industrial waste by Table vibratory test, standard and modified Proctor test.

Table 2.8 MDD as per different tests; Vibratory, Standard, Modified Proctor test

	Vibratory Test	Standard Proctor	Modified Proctor
Sample	Maximum density (gm/cc)	Maximum density (gm/cc)	Maximum density (gm/cc)
Sand	1.51	1.49	1.66
Fly ash	1.19	1.29	1.40
Red mud	2.14	2.05	2.15
Crusher dust	2.02	2.04	2.11
Slag	2.05	2.04	2.16

4. DIRECT SHEAR TEST

Figure 2.12 gives a cohesion value of .31 kN/m² and angle of friction of 38.52° for sand.

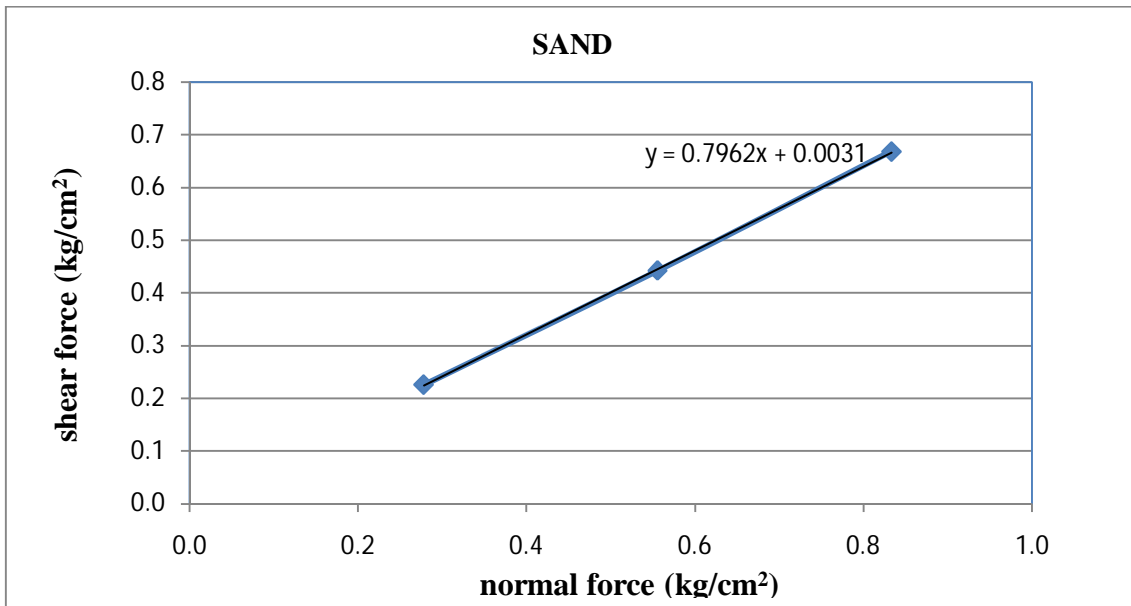


Fig. 2.11 Direct shear test for Sand

Figure 2.13 gives a cohesion value of 19.68 kN/m² and angle of friction of 24.37° for fly ash.

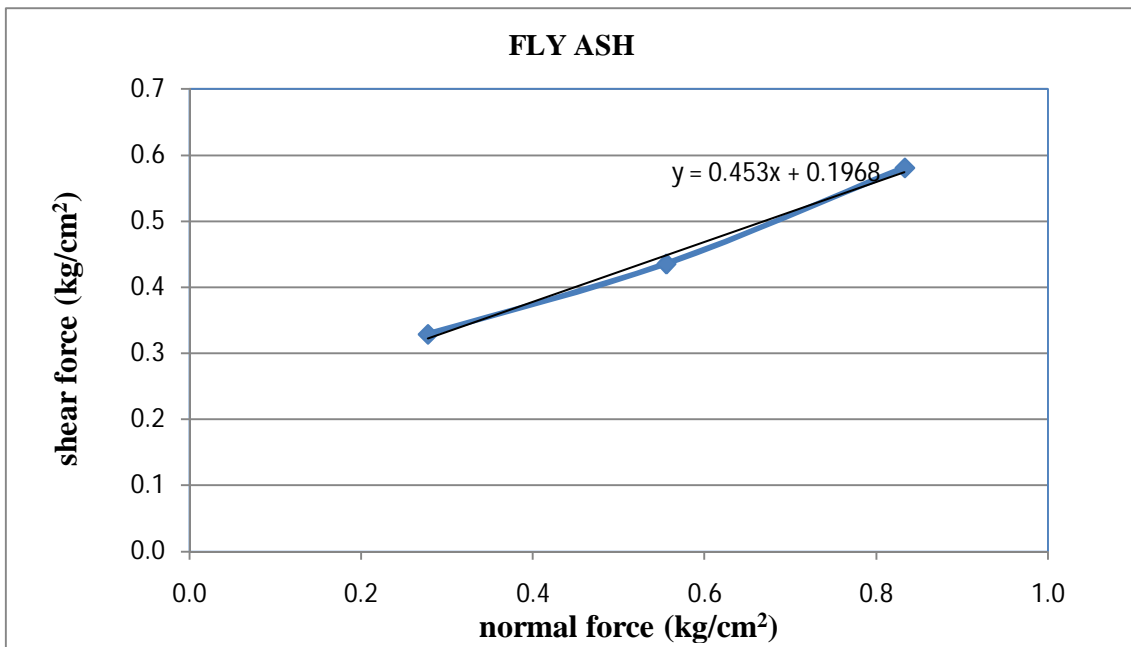


Fig. 2.12 Direct shear test for Fly ash

Figure 2.14 gives a cohesion value of 13.87 kN/m² and angle of friction of 26° for red mud.

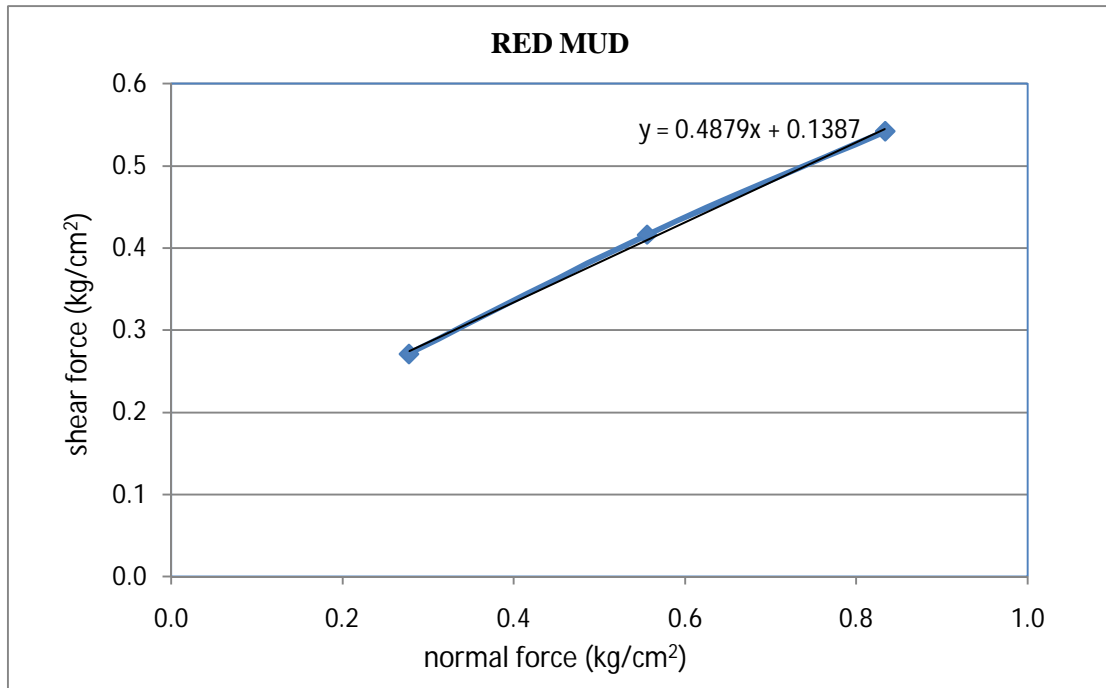


Fig. 2.13 Direct shear test for Red mud

Figure 2.15 gives a cohesion value of 0.31 kN/m² and angle of friction of 27.7° for crusher dust.

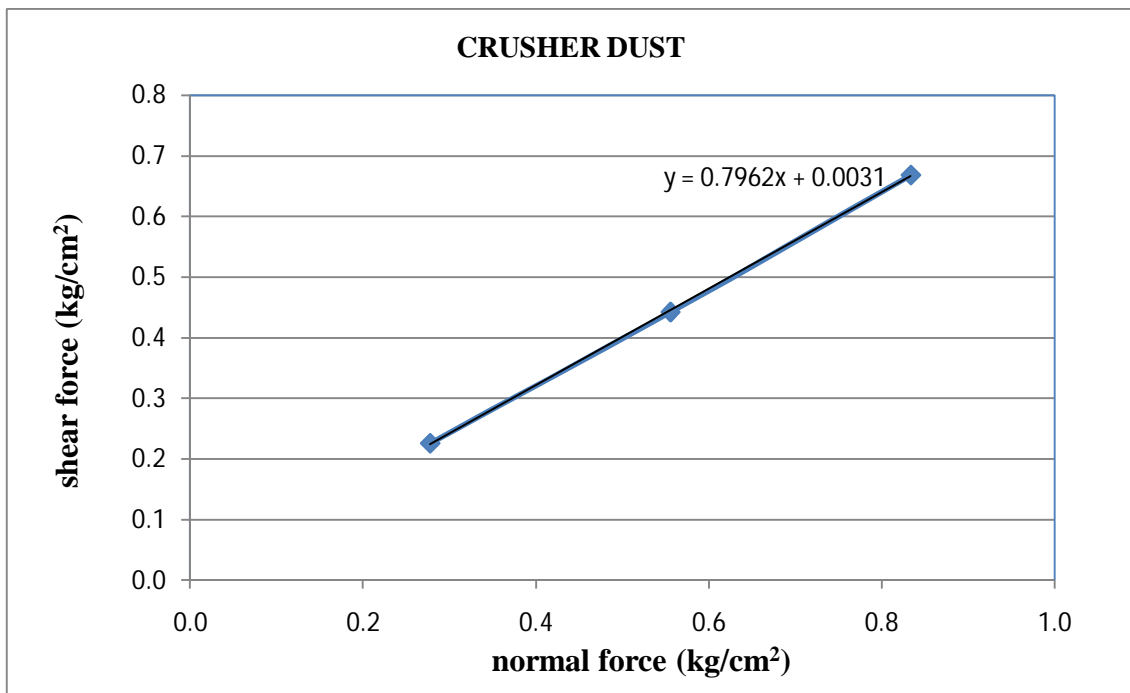


Fig. 2.14 Direct shear test for Crusher dust

Figure 2.16 gives a cohesion value of 0.94 kN/m² and angle of friction of 34.77° for slag.

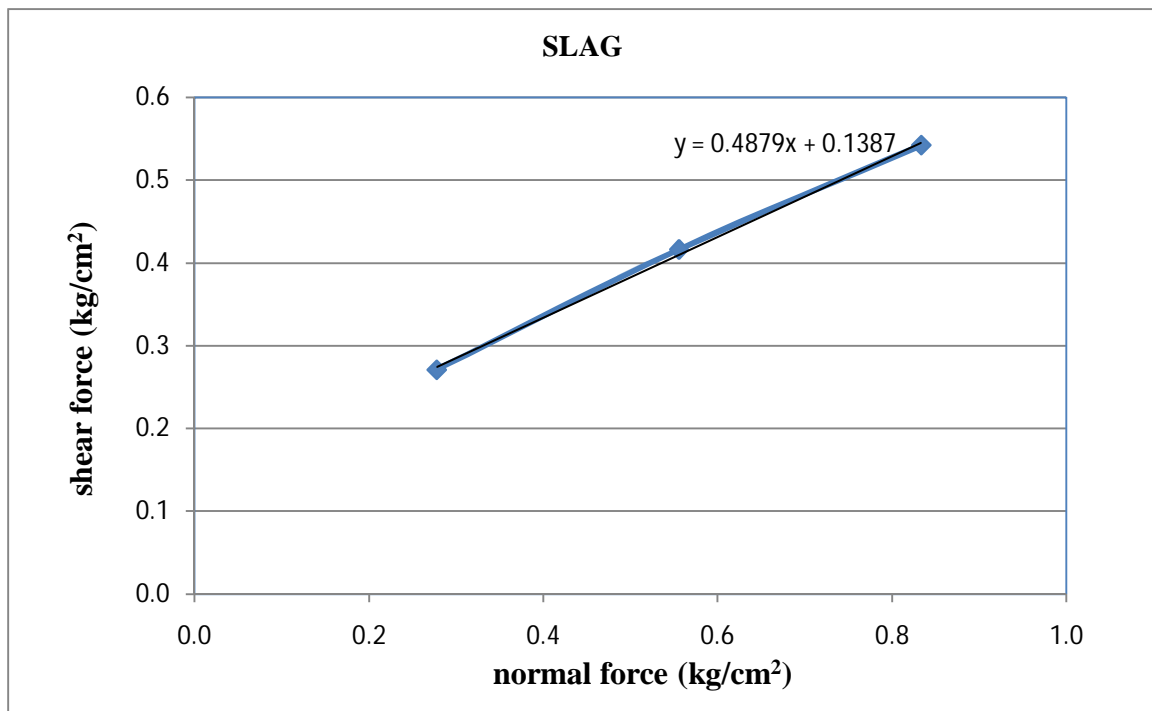


Fig. 2.15 Direct shear test for Slag

Table 2.9 Cohesion, Angle of friction for different materials

MATERIALS	Cohesion (kN/m ²)	Angle of Friction (Degrees)
SAND	0.31	38.52
FLY ASH	19.68	24.37
RED MUD	13.87	26.00
CRUSHER DUST	0.31	27.70
SLAG	0.94	34.77

From Table 2.9 it can be seen that angle of friction of sand is highest among all the material used in the experiment, while fly ash has the lowest angle of friction.

CHAPTER-3

FINITE ELEMENT ANALYSIS OF FOUNDATIONS AND RETAINING WALLS

3.1 METHOD OF ANALYSIS

FINITE ELEMENT METHOD:

The finite element Method has been used in many fields of engineering over forty years. The finite element method is a significant aspect of soil mechanics to predict soil behaviour by constitutive equations. This allows engineers to solve various types of geotechnical engineering problems, especially problems that are inherently complex and cannot be solved using traditional analysis without making simplified assumptions. To simulate the exact behaviour of soil, various soil models have been developed and to simplify the analysis procedure various software packages have been developed.

PLAXIS:

Plaxis is Finite Element Software Developed at the Technical University of Delft for Dutch Government. Initially was intended to analyze the soft soil river embankments of the lowlands of Holland. Soon after, the company Plaxis BV was formed, and the program was expanded to cover a broader range of geotechnical issues. The Plaxis programme started at Delft University of Technology in early 1970's when Peter Vermeer started to do a programme of research on finite element analysis on the design and construction of Eastern Scheldt Storm-Barrier in Netherland. Initial finite element code was developed to calculate the elastic-plastic plane using six-nodded triangular elements, written in Fortran VV. In the year 1982 Rene de Borst under the supervision of Pieter Vermeer ,performed his master's programme related topic on the analysis of cone penetration test in clay. The study of axisymmetric led to the existence of Plaxis.

The study was on six-nodded triangles in the element. This 15 – noded triangle was developed thus increasing the number of nodes in the element. The usage of 15-noded triangle is the simplest element for any analysis in axisymmetric. Then the experts De Borst and Vermeer

implement the 15-noded triangle in Plaxis thus solving the problem of cone penetrometer. The development of Plaxis proceeds with the problem to solve the soil structure interaction effects. This led to the study on beam element by Klaas Bakker under the supervision of Pieter Vermeer. The outcome of the experiment using beam element was applicable to flexible retaining wall and later application to the analysis of flexible footings and rafts. Baker's work formulated the implementation of 5-noded beam element in Plaxis (Bakker et al (1990), Bakker et al (1991)). The 5-noded beam element is compatible to the 15-noded triangular elements (has 5 nodes). Baker's work was novel for the invention of hybrid method introducing the displacement of degree-of-freedom to the element behaviour. The lack of degree of freedom has made solution to reduce the number of variables thus simplified the element.

Seismic condition:

The effect of pseudo-static horizontal earthquake body forces on the bearing capacity of foundations on sloping ground has been assessed using Finite Element Method. Two failure mechanisms were considered, based on the extension of the characteristics from the ground surface towards the footing base from either onside or both sides. The magnitude of N_γ based on the both-sides failure mechanism, for smaller values of earthquake acceleration coefficient (α_h), has been found to be significantly smaller than that obtained using the single side mechanism; however, in the presence of α_h the both sides mechanism becomes kinematically inadmissible in many cases for higher values of ϕ . Only the single-side mechanism was found statically admissible for computing the bearing capacity factors N_c and N_q on sloping ground.

All the bearing capacity factors reduce considerably with increase in α_h for various ground inclinations.

PROBLEM DEFFINATION:

In hilly terrain it is necessary to have footing on the slope or on the sloping ground. The figure below shows a typical case for the same.



Fig. 3.1 Typical case of footing on hilly terrain

In the present study the above field problem has been analyzed for both static and seismic condition. The figure below shows the schematic diagram for the present study.

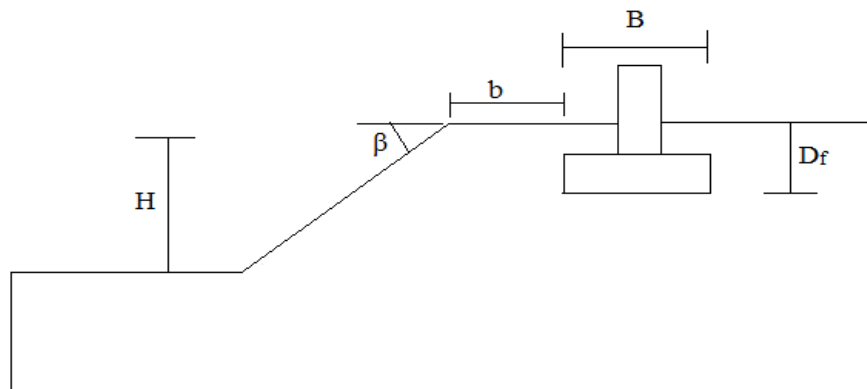


Fig. 3.2 Schematic diagram of field problem

It has been seen that limited studies have been carried out for the footings embedded in sloping ground and that too using Limit Equilibrium or Analytical Method. In the present study Finite Element Method is used which is more precise and gives more accurate result

EXAMPLES:

The objective of this study is to determine the ultimate bearing capacity of a shallow continuous footing with width B in the presence of horizontal earthquake acceleration $\alpha_h g$ (g is the acceleration due to gravity). The footing is placed horizontally on an inclined ground surface having an inclination β with the horizontal. It is assumed that the ground surface is loaded with a layer of soil overburden having equal vertical thickness, d , on either side of the footing. Figure 3.3 shows the geometry of the inclined ground with footing.

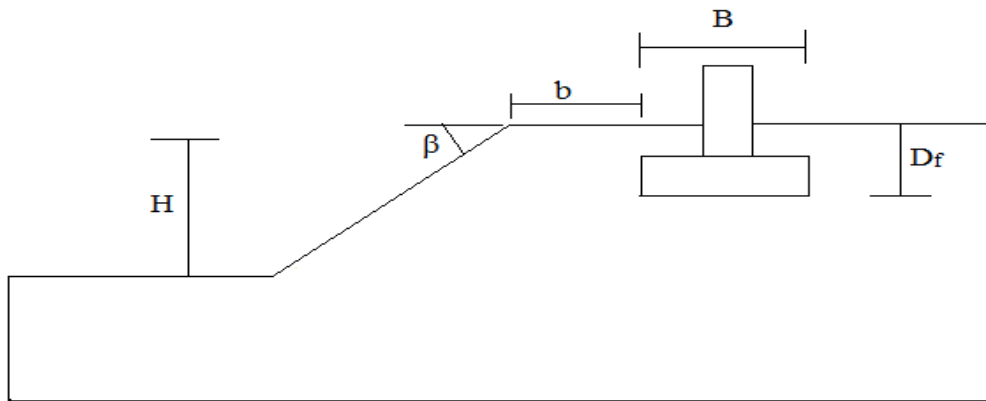


Fig. 3.3 Geometry of inclined ground with embedded footing

Data Given:

Width of Footing $B = 2$ m

Depth of Footing $D_f = 2$ m

Height of the slope $H = 6.2$ m

Angle of inclination β (varies for different cases)

Distance from top of slope to foundation $b = 1.2$ m

Unit weight of soil $= 17.5$ KN/m³

Angle of Friction $\phi = 30^\circ$

Cohesion $c = 50$ KN/m²

STATIC LOADING

CASE 1: ($\beta = 15^\circ$)

The Figure below shows the geometry of the sloping ground with embedded footing for an angle of inclination of 15° .

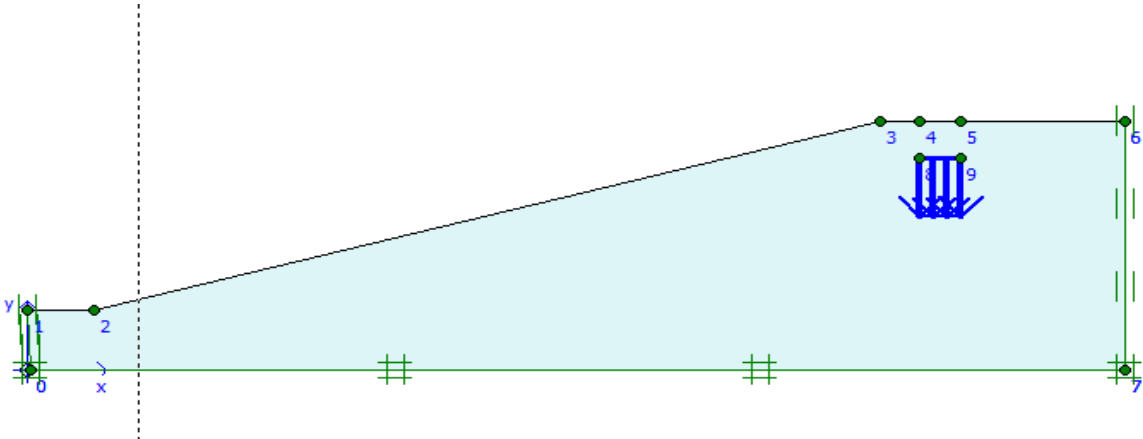


Fig. 3.4 Geometry of embedded footing for angle of inclination of 15°

The figure below shows the settlement of soil for the above geometry for the standard prescribed displacement of 50mm

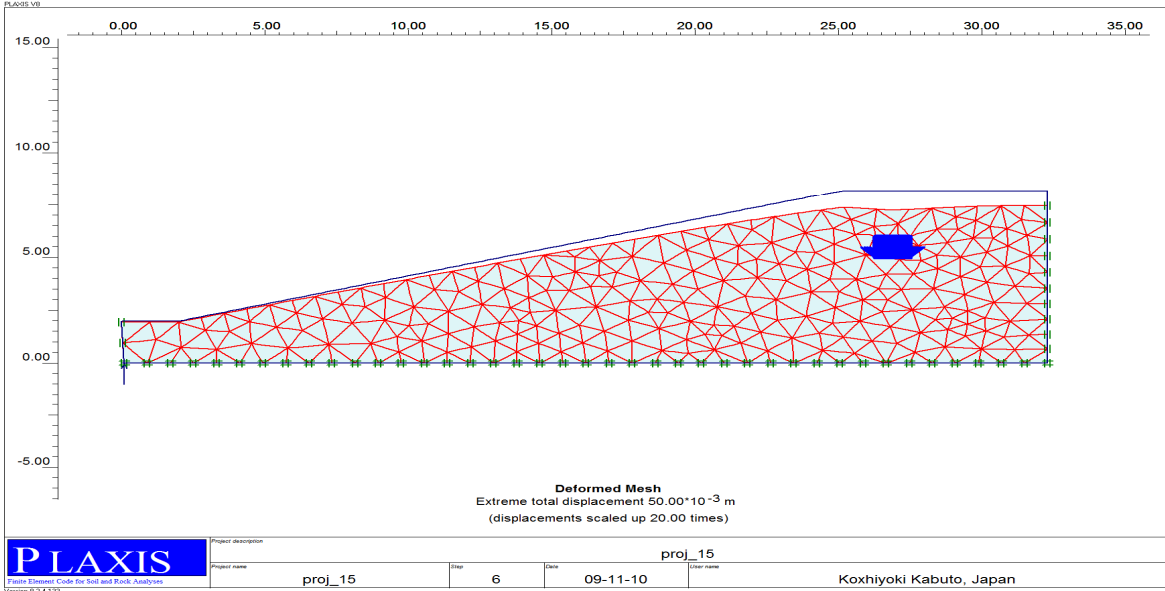


Fig. 3.5 Settlement of soil for Case-1 (static load)

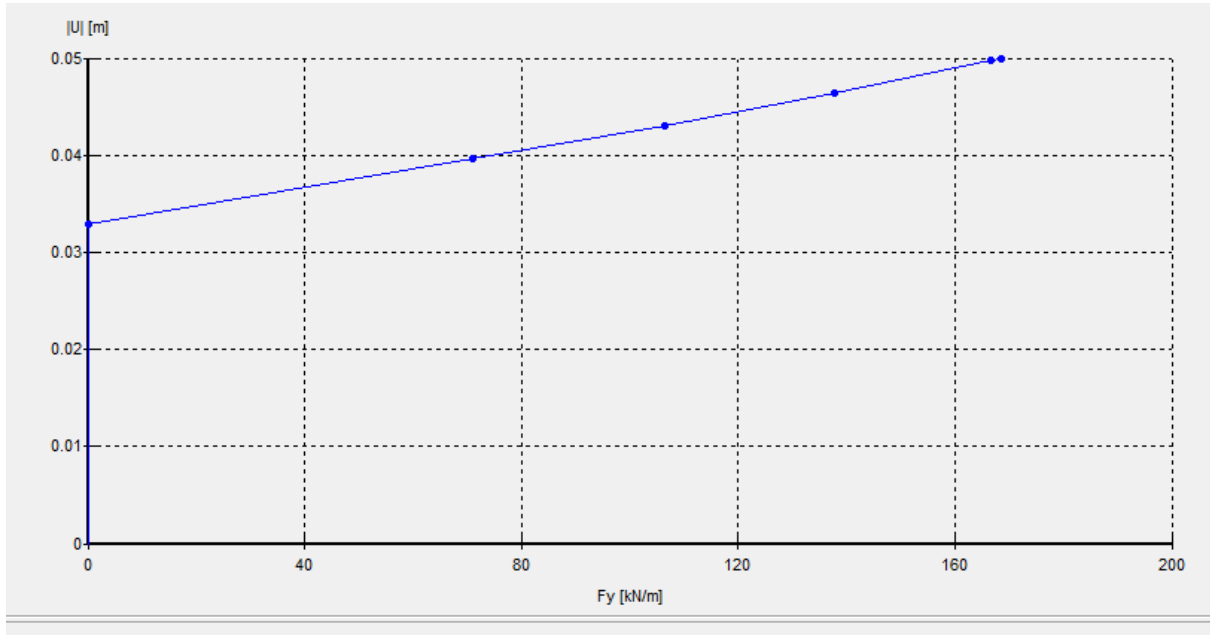


Fig. 3.6 Force Vs Displacement graph for Case-1 (static load)

Ultimate load bearing capacity for the above footing is found to be **168.68 kN/m²**

CASE 2: ($\beta = 30^\circ$)

The Figure below shows the geometry of the sloping ground with embedded footing for an angle of inclination of 30° .

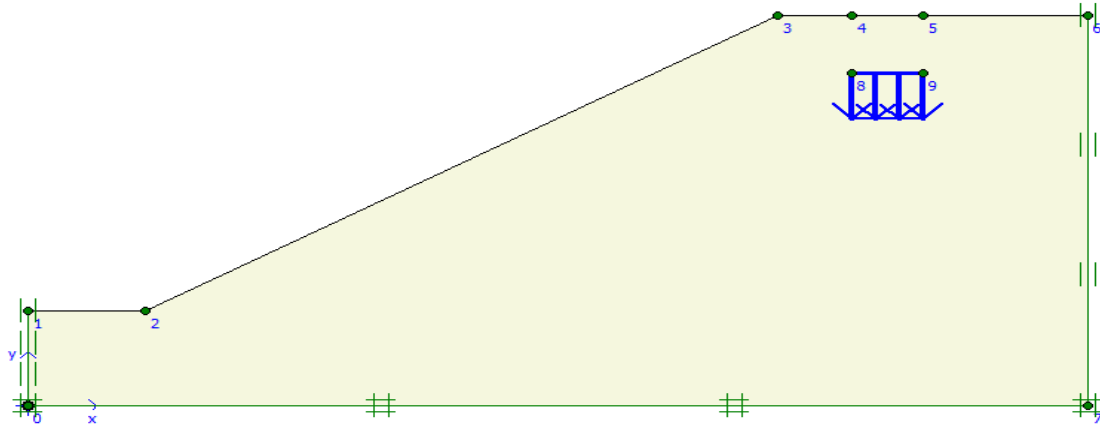


Fig. 3.7 Geometry of embedded footing for angle of inclination of 30°

The figure below shows the settlement of soil for the above geometry for the standard prescribed displacement of 50mm

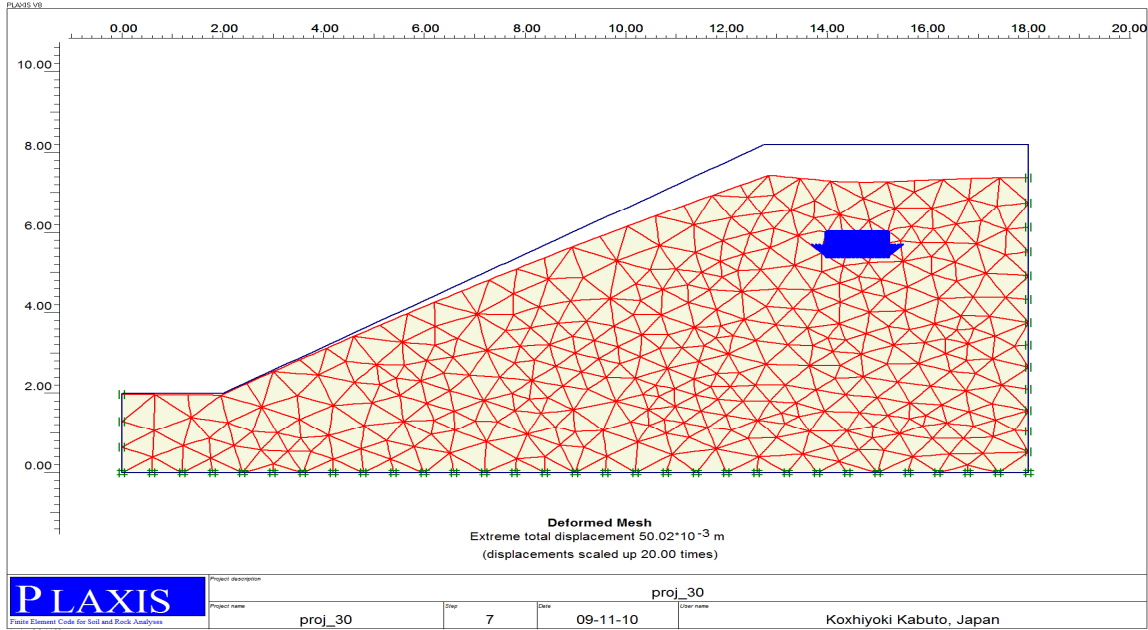


Fig. 3.8 Settlement of soil for Case-2 (static load)

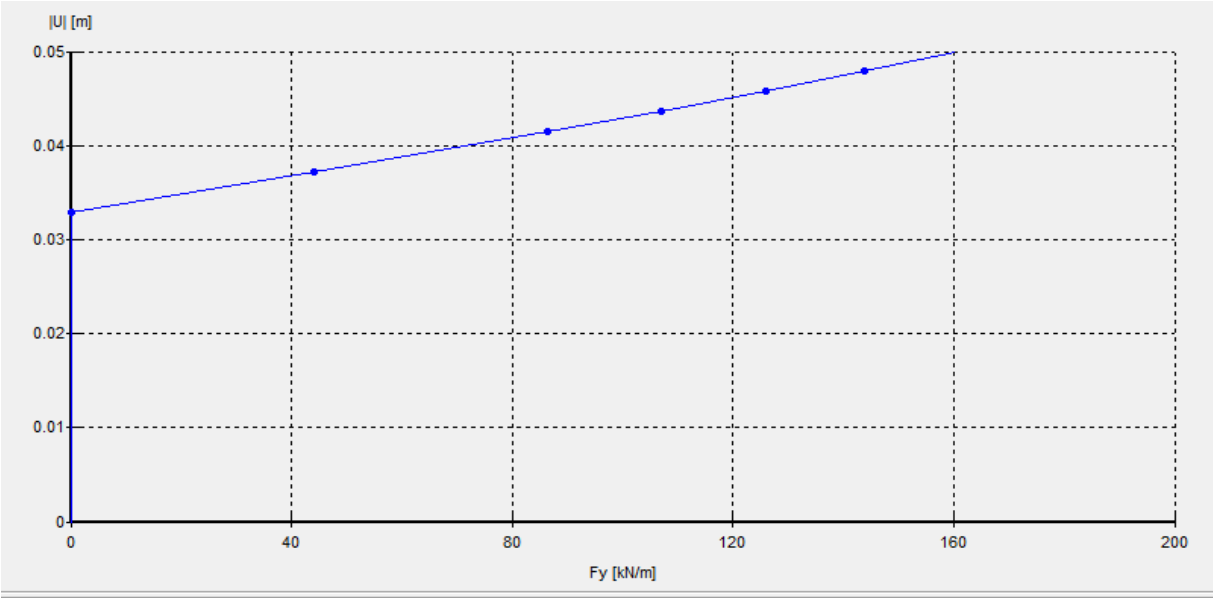


Fig. 3.9 Force Vs Displacement graph for Case-2 (static load)

Ultimate load bearing capacity for the above footing is found to be **160.37 kN/m²**

CASE 3: ($\beta = 60^\circ$)

The Figure below shows the geometry of the sloping ground with embedded footing for an angle of inclination of 60° .

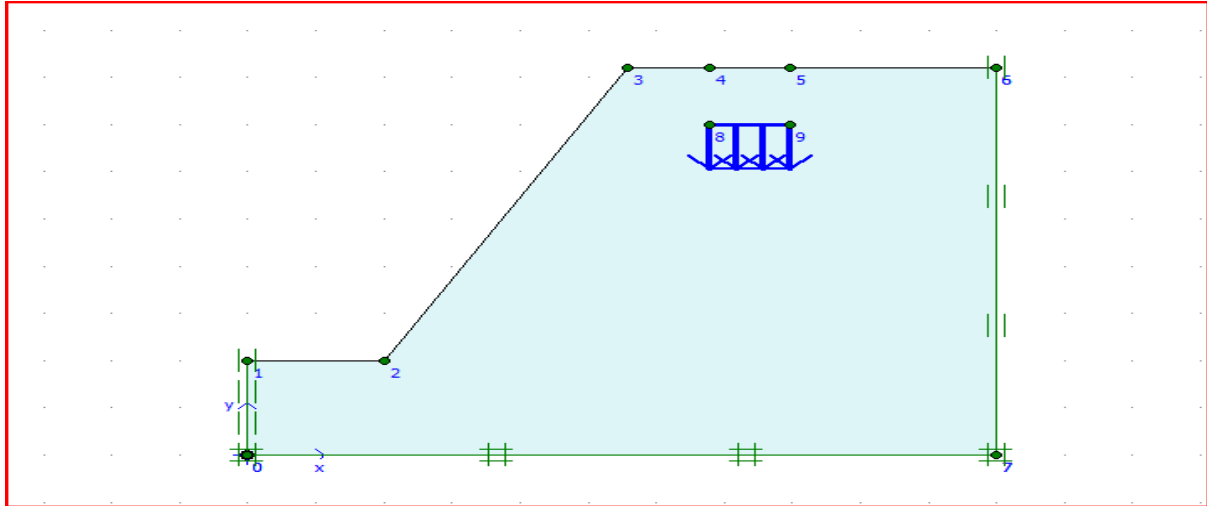


Fig. 3.10 Geometry of embedded footing for angle of inclination of 60°

The figure below shows the settlement of soil for the above geometry for the standard prescribed displacement of 50mm

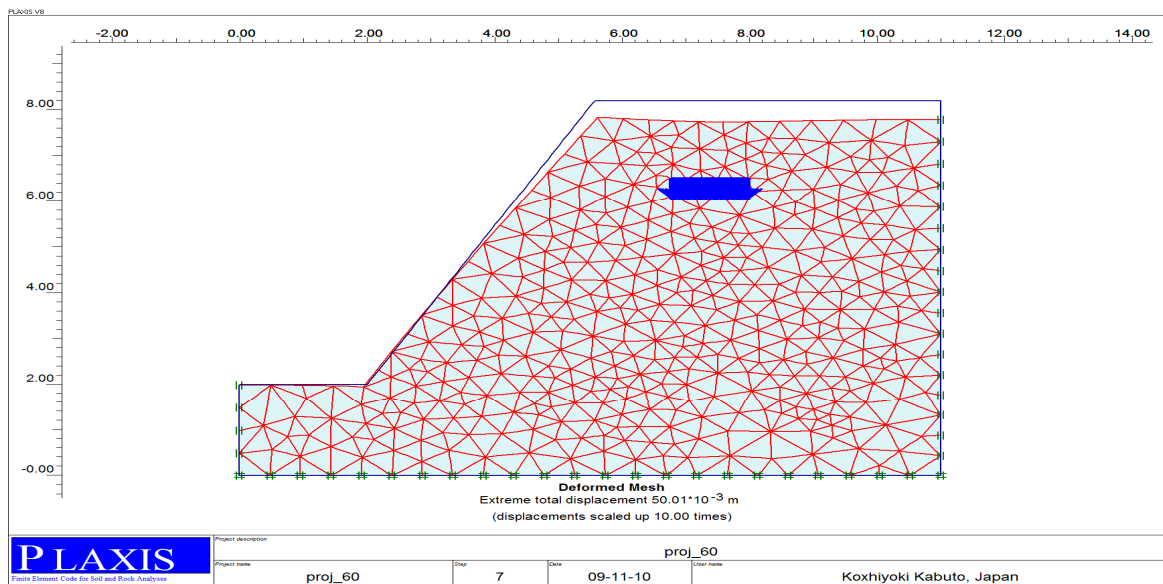


Fig. 3.11 Settlement of soil for Case-3 (static load)

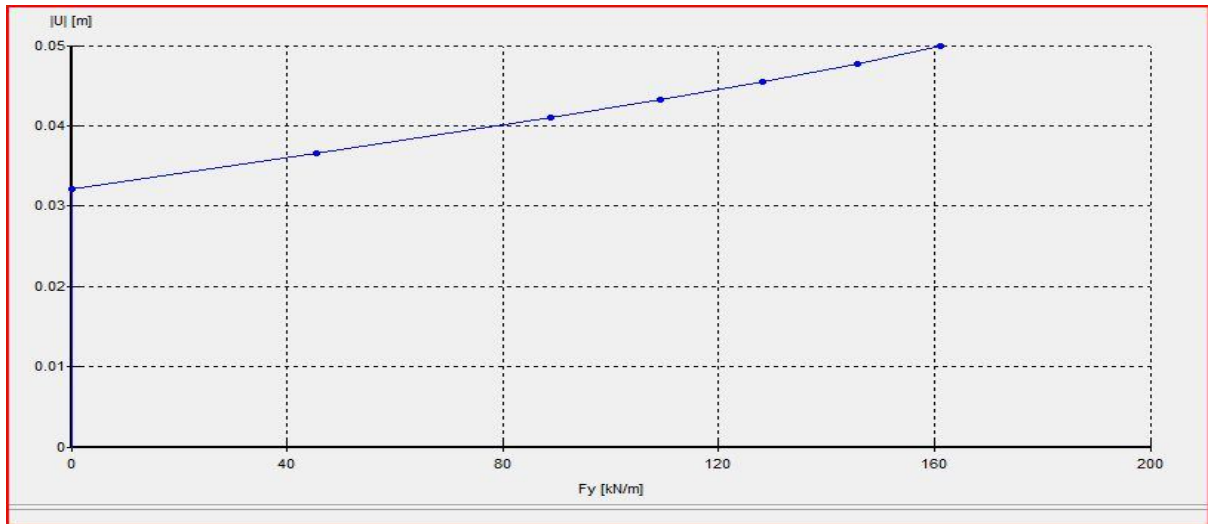


Fig. 3.12 Force Vs Displacement graph for Case-3 (static load)

Ultimate load bearing capacity for the above footing is found to be **156.17 kN/m²**

SEISMIC LOAD:

CASE 1: ($\beta = 15^\circ$ Horizontal acceleration = 0.1g)

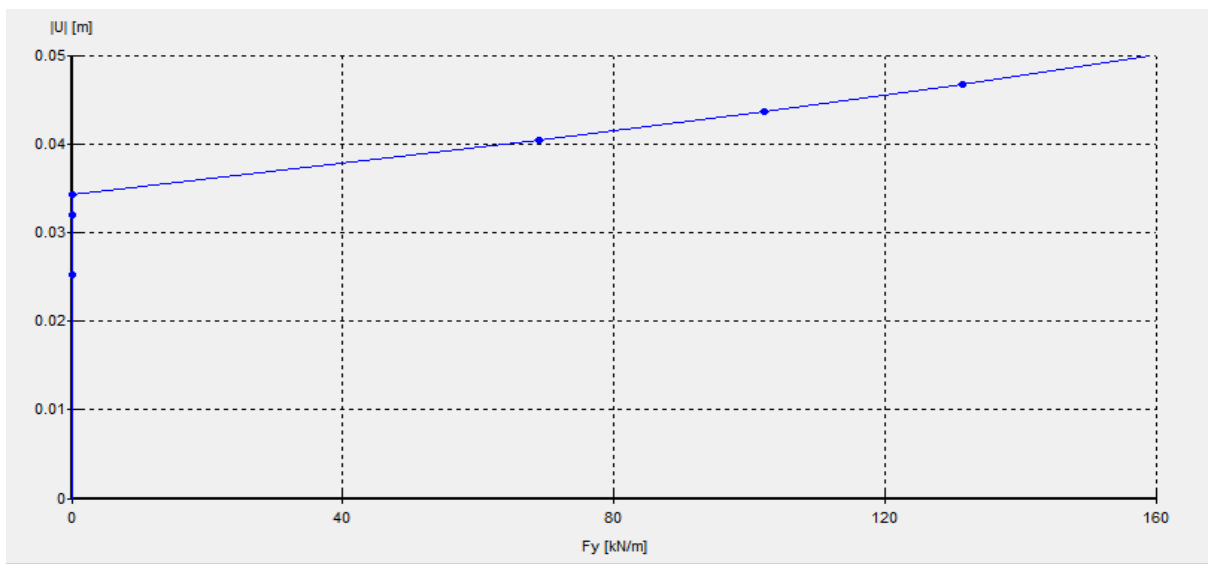


Fig. 3.13 Force Vs Displacement graph for Case-1 (seismic load)

Ultimate load bearing capacity for the above footing is found to be **157.88 kN/m²**

CASE 2: ($\beta = 15^\circ$ Horizontal acceleration = 0.2g)

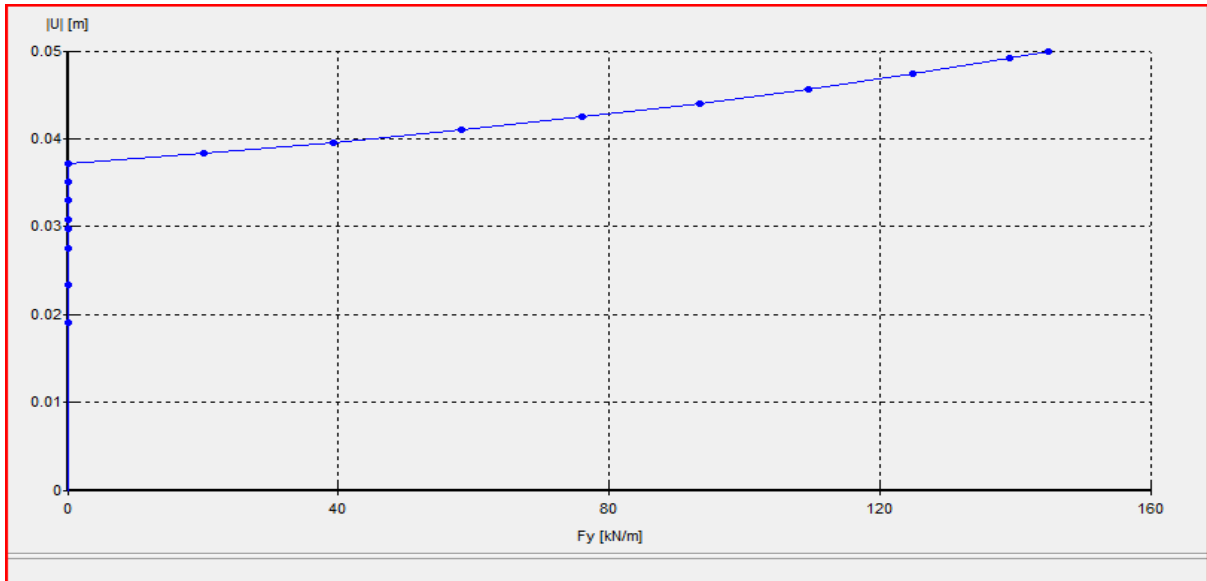


Fig. 3.14 Force Vs Displacement graph for Case-2 (seismic load)

Ultimate load bearing capacity for the above footing is found to be **154.65 kN/m²**

CASE 3: ($\beta = 30^\circ$ Horizontal acceleration = 0.1g)

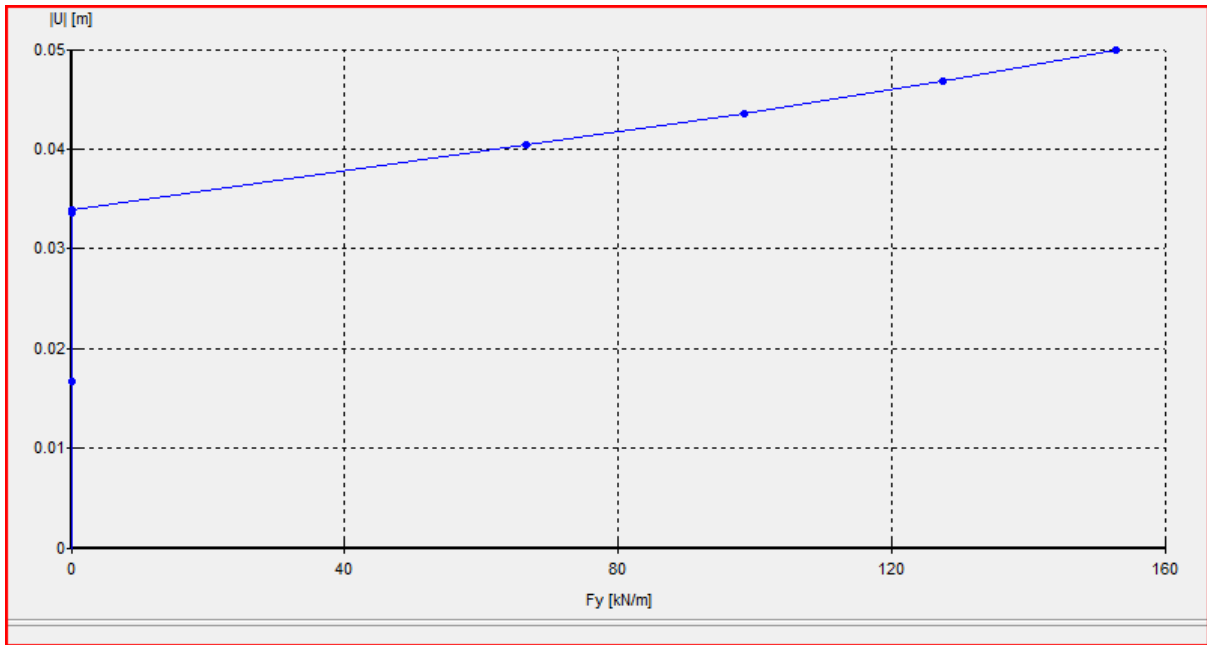


Fig. 3.15 Force Vs Displacement graph for Case-3 (seismic load)

Ultimate load bearing capacity for the above footing is found to be **152.57 kN/m²**

CASE 4: ($\beta = 30^\circ$ Horizontal acceleration = 0.2g)

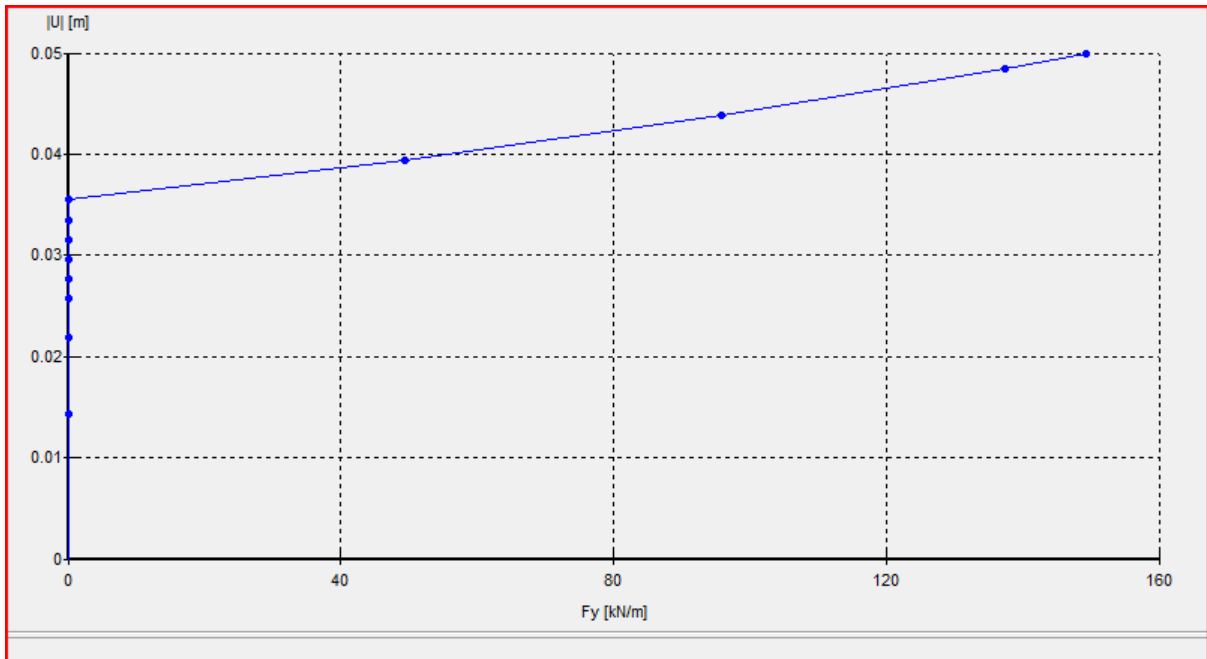


Fig. 3.16 Force Vs Displacement graph for Case-4 (seismic load)

Ultimate load bearing capacity for the above footing is found to be **149.23 kN/m²**

CASE 5: ($\beta = 60^\circ$ Horizontal acceleration = 0.1g)

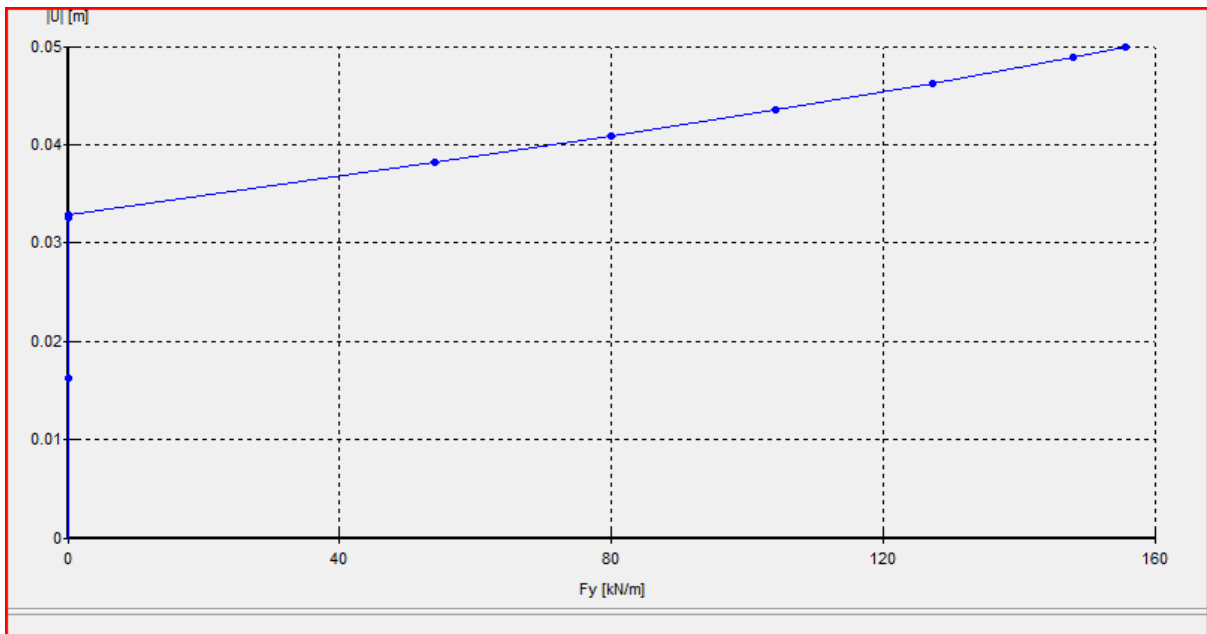


Fig. 3.17 Force Vs Displacement graph for Case-5 (seismic load)

Ultimate load bearing capacity for the above footing is found to be **150.56 kN/m²**

CASE 6: ($\beta = 60^\circ$ Horizontal acceleration = 0.2g)

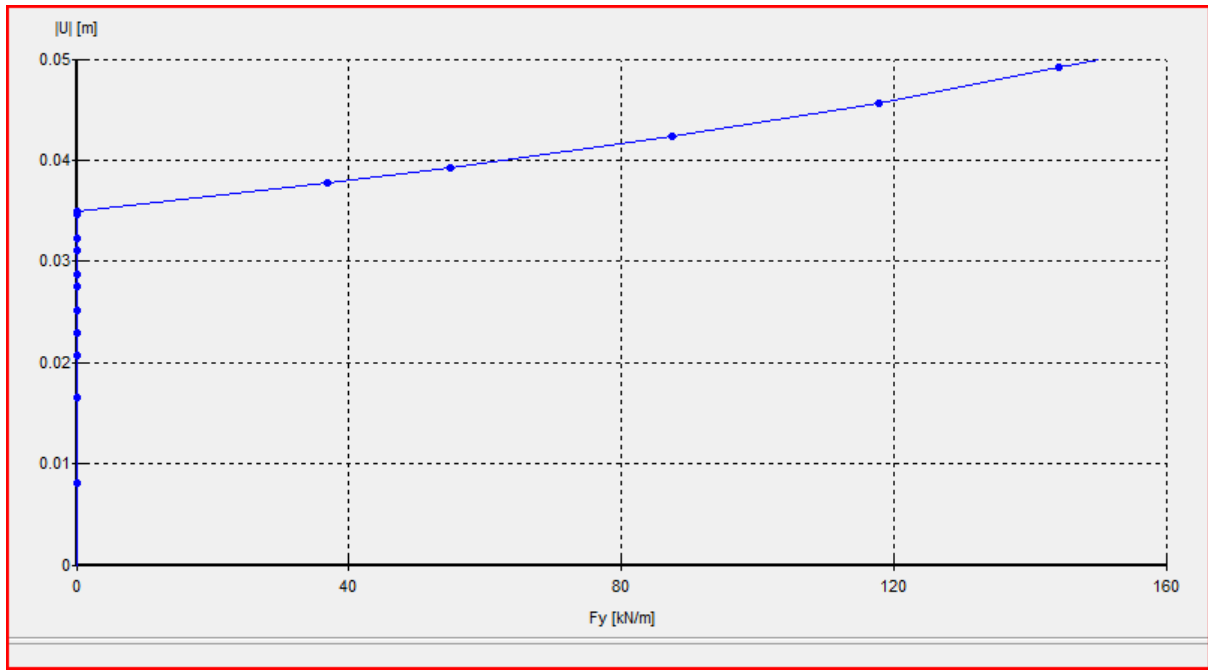


Fig. 3.18 Force Vs Displacement graph for Case-6 (seismic load)

Ultimate load bearing capacity for the above footing is found to be **148.79 kN/m²**

From the above case results, it can be concluded that

1. With increase in angle of inclination of slope the ultimate load bearing capacity of footing decreases i.e. the footing fails at lower value of load.
2. Introduction of horizontal earthquake acceleration i.e. seismic load the structure fails at lower value of load as compare to the structure without seismic load.

In our case study we have taken the dimensions as mentioned below:

$L=20$ m, $L_1=12$ m

$H=12$ m and $H_1=6$ m

The properties of the foundation soil are as follows:

Material model: Linear elastic

$\gamma_{\text{unsat}}=18$ kN/m³ , $\gamma_{\text{sat}}=20$ kN/m³

Co-efficient of elasticity, $E= 100000$ kN/m²

The properties of plate retaining wall:

Material type: Elastic

$EA= 3*10^7$ kN/m, $EI= 5*10^7$ kN/m²/m, Poisson's ratio= 0.15

The aim is to find out the effective earth pressure on the retaining wall due to back fill. In the back fill we used the industrial wastes such as fly ash, slag, crusher dust and red mud.

1. Sand as backfill

Figure 3.20 shows the deformed mess of retaining wall when sand is used as backfill

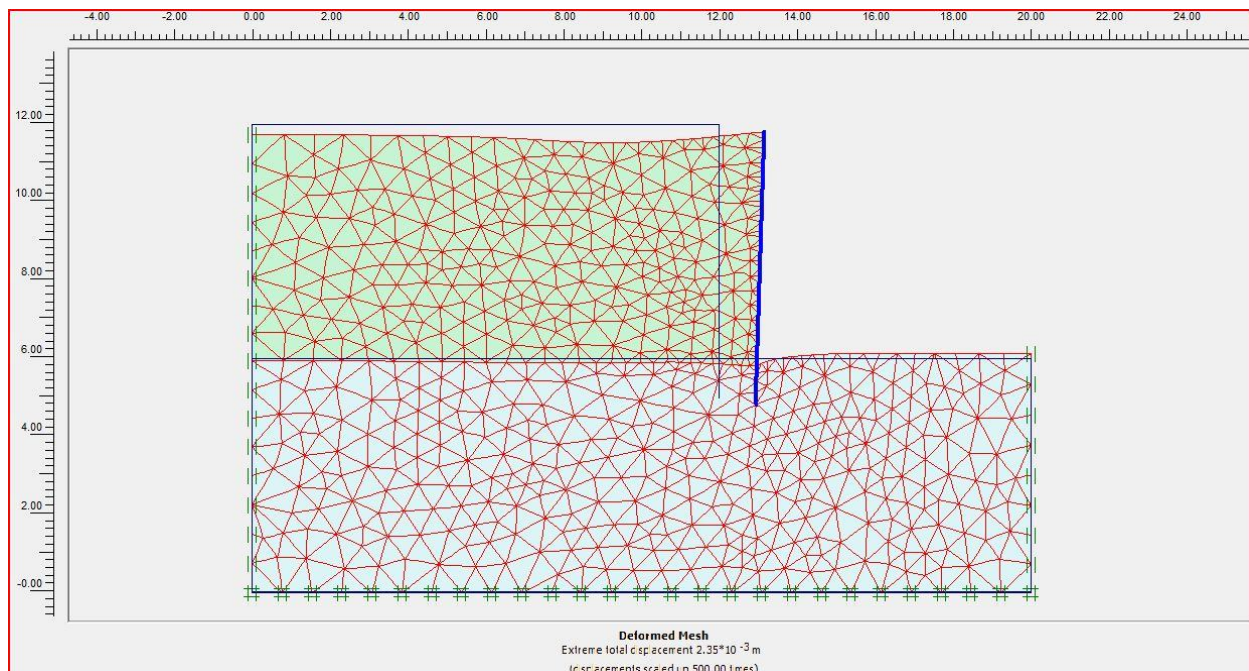


Fig 3.20 Deformed mesh of retaining wall for sand

Figure 3.21 shows the distribution of the active earth pressure on the retaining wall when sand is used as backfill.

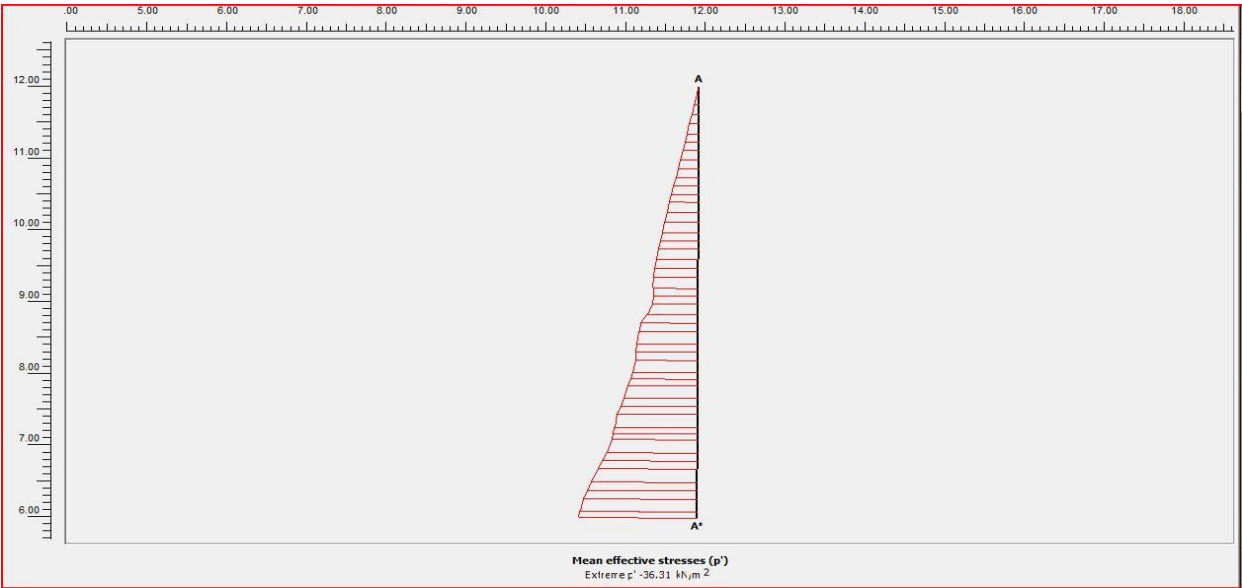


Fig 3.21 Distribution of effective stress on retaining wall by sand

2. Fly ash as backfill

Figure 3.22 shows the deformed mesh of retaining wall when fly ash is used as backfill

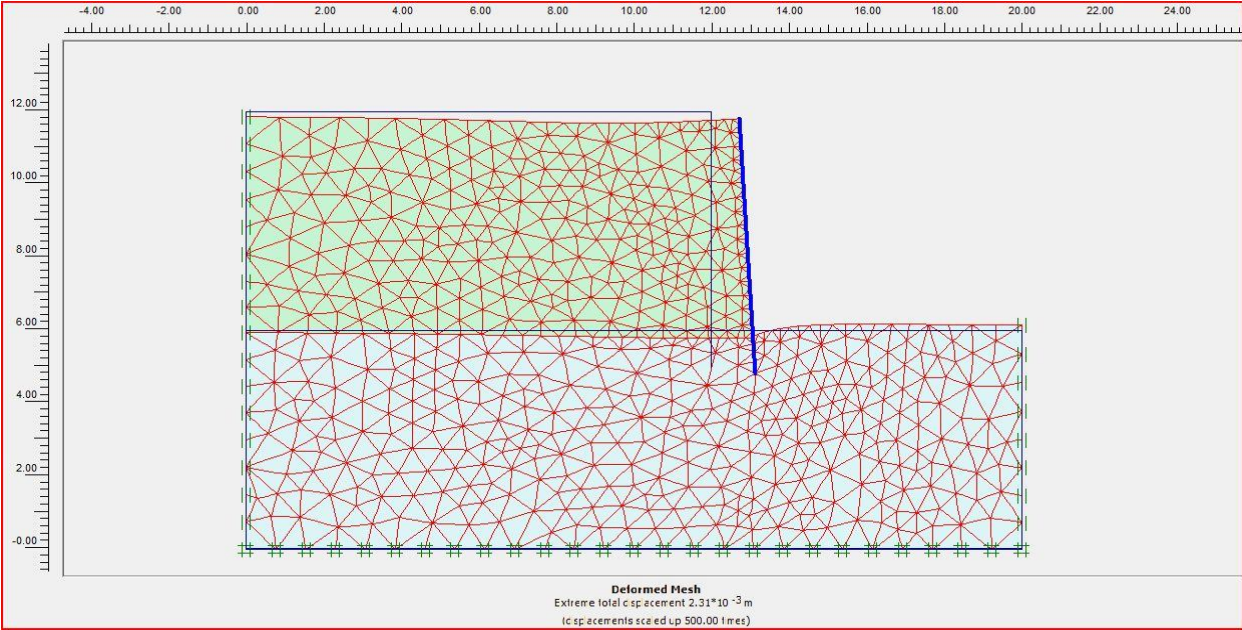


Fig 3.22 Deformed mesh of retaining wall for fly ash

Figure 3.23 shows the distribution of the active earth pressure on the retaining wall when fly ash is used as backfill.

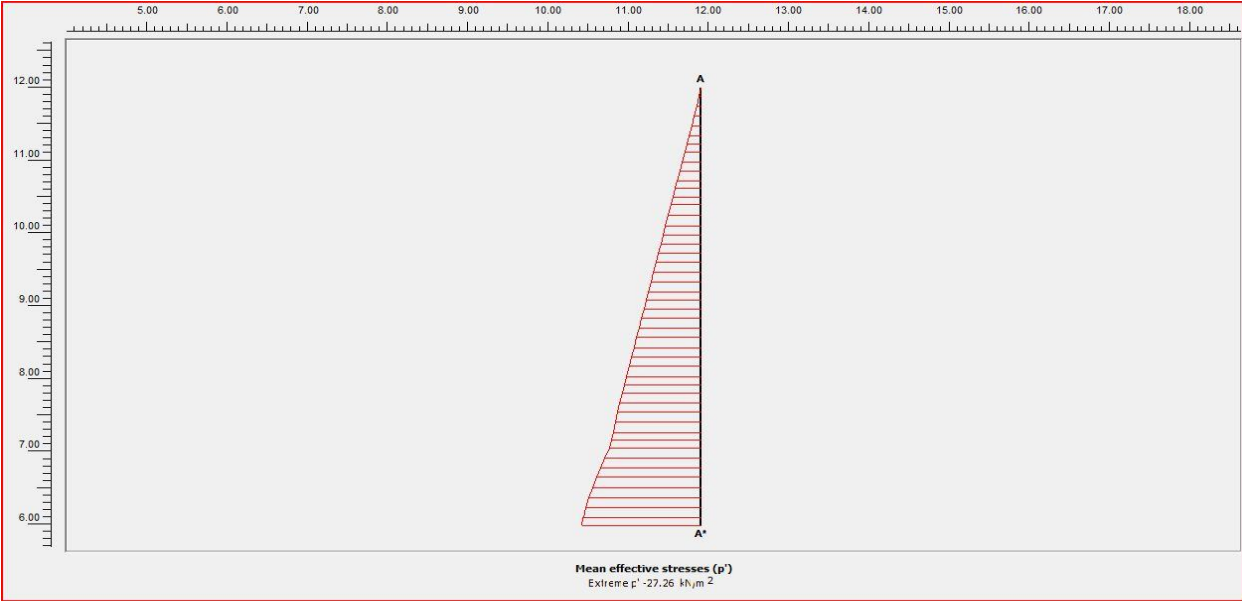


Fig 3.23 Distribution of effective stress on retaining wall by fly ash

3. Red mud as backfill

Figure 3.24 shows the deformed mesh of retaining wall when red mud is used as backfill

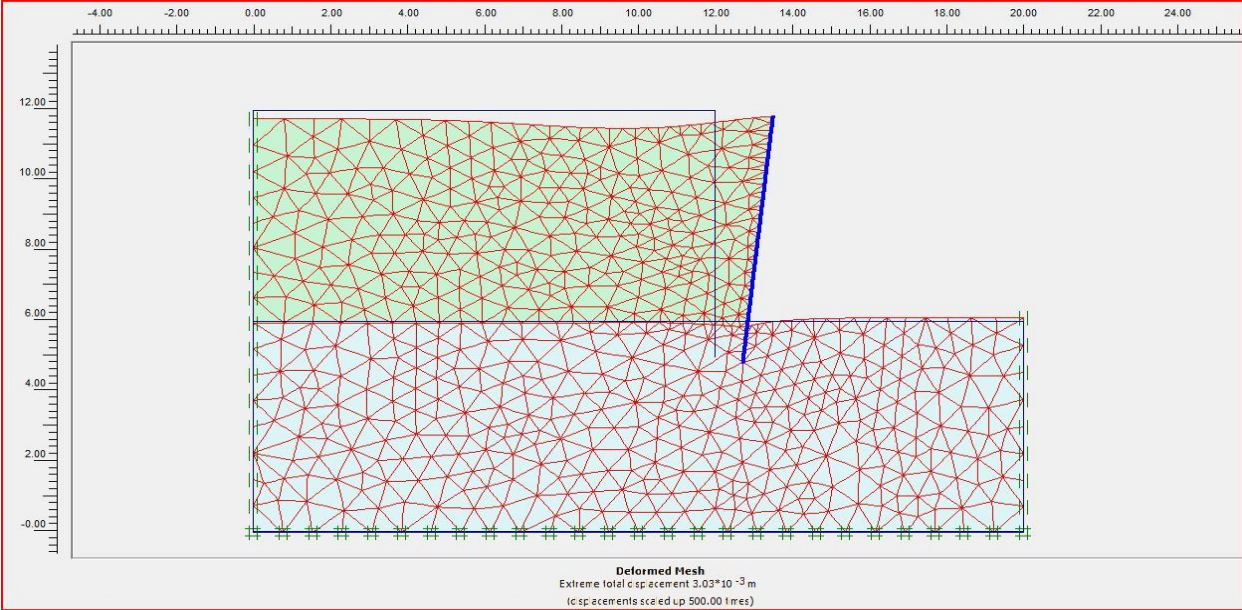


Fig 3.24 Deformed mesh of retaining wall for red mud

Figure 3.25 shows the distribution of the active earth pressure on the retaining wall when red mud is used as backfill.

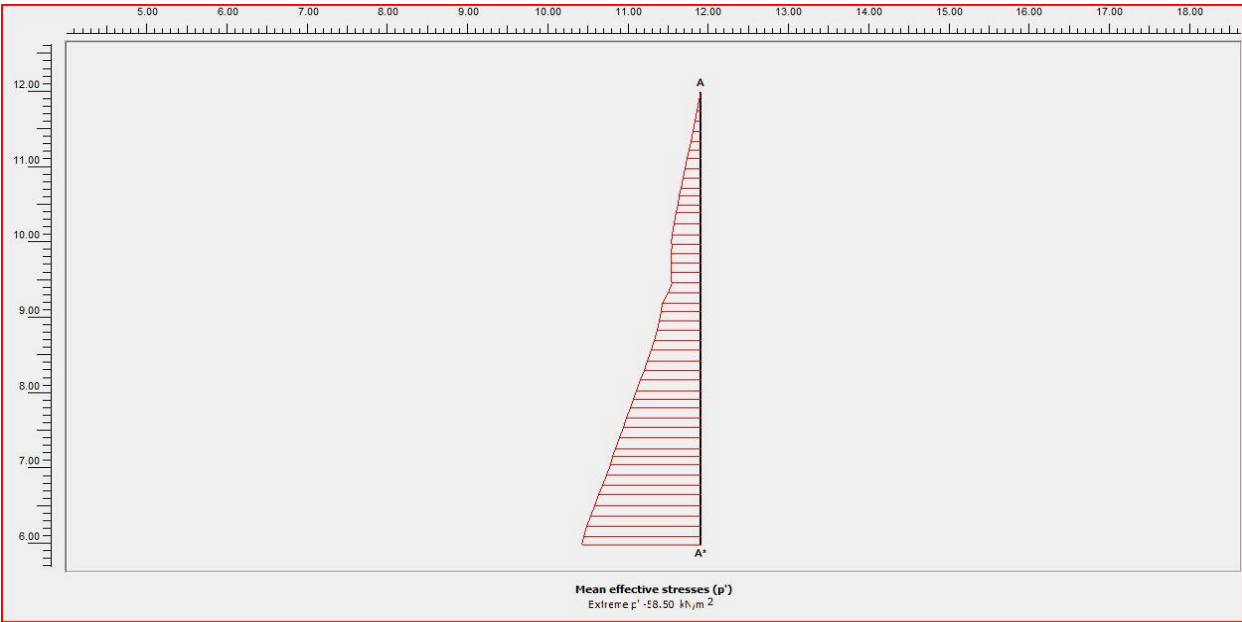


Fig 3.25 Distribution of effective stress on retaining wall by red mud

4. Crusher dust as backfill

Figure 3.26 shows the deformed mesh of retaining wall when crusher dust is used as backfill

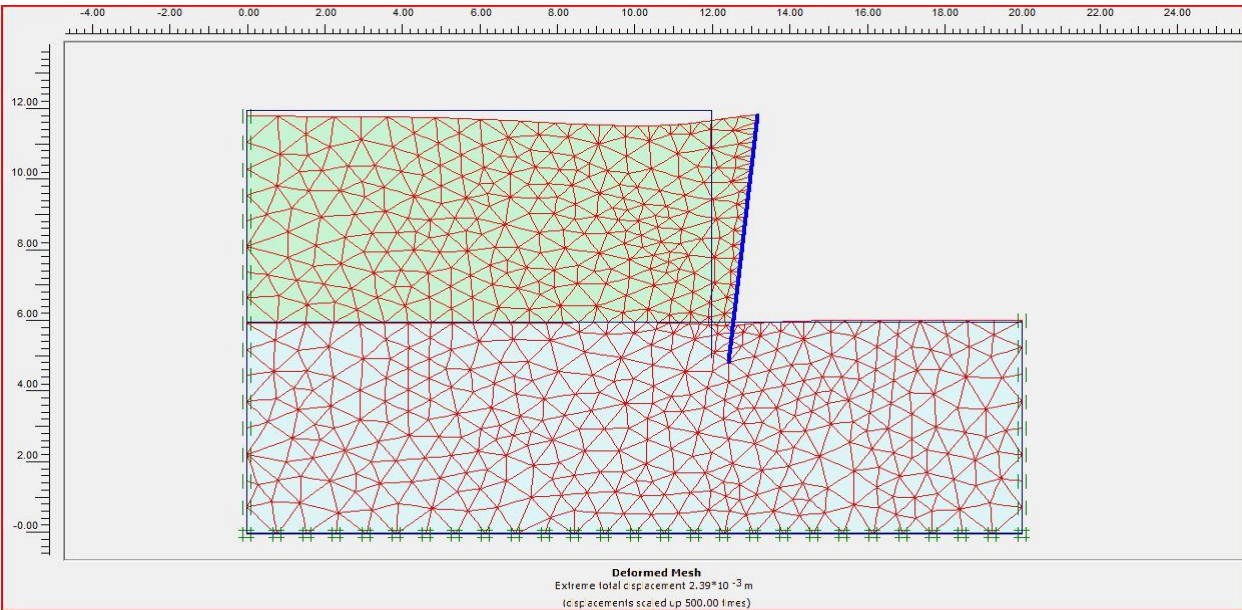


Fig 3.26 Deformed mesh of retaining wall for crusher dust

Figure 3.27 shows the distribution of the active earth pressure on the retaining wall when crusher dust is used as backfill.

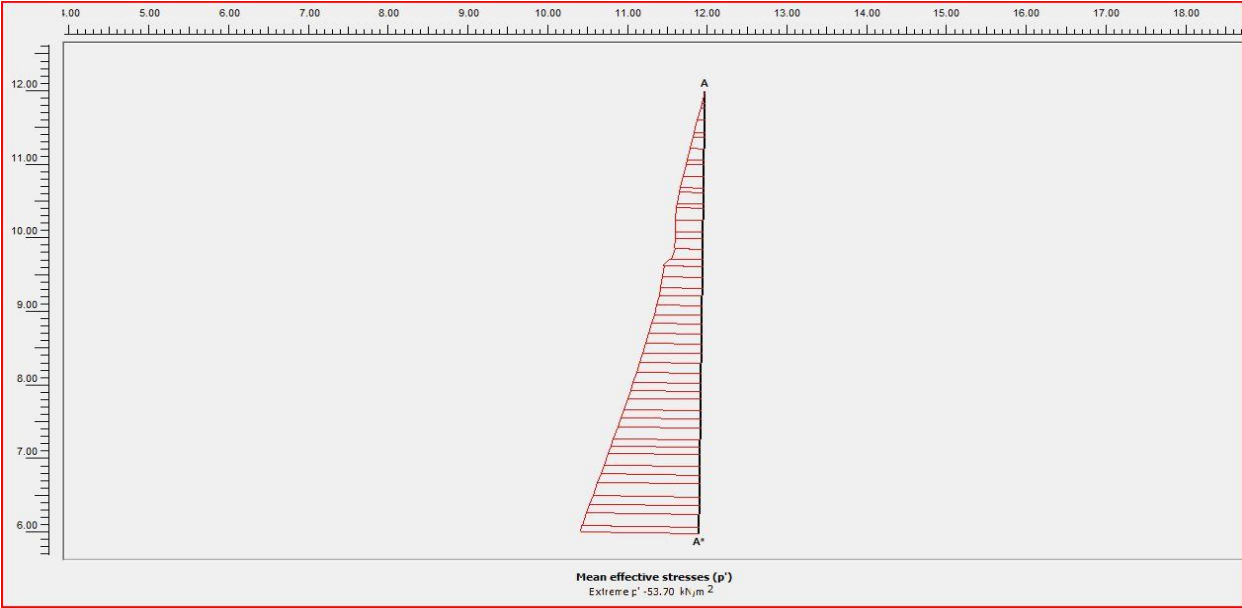


Fig 3.27 Distribution of effective stress on retaining wall by crusher dust

5. Slag as backfill

Figure 3.28 shows the deformed mesh of retaining wall when slag is used as backfill

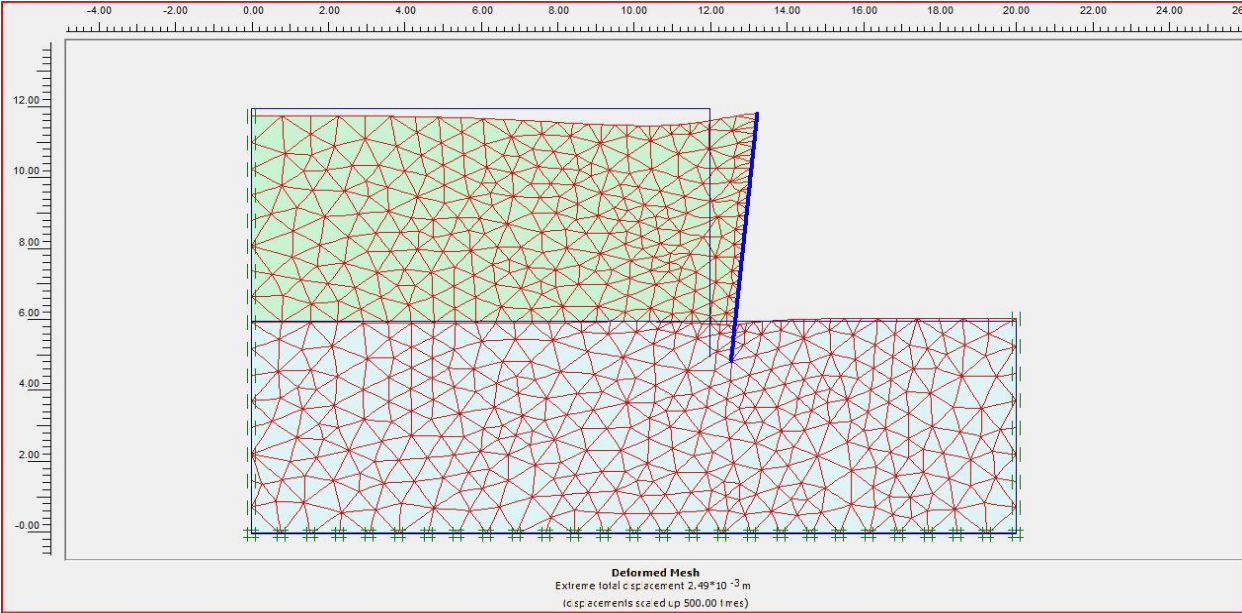


Fig 3.28 Deformed mesh of retaining wall for slag

Figure 3.29 shows the distribution of the active earth pressure on the retaining wall when slag is used as backfill.

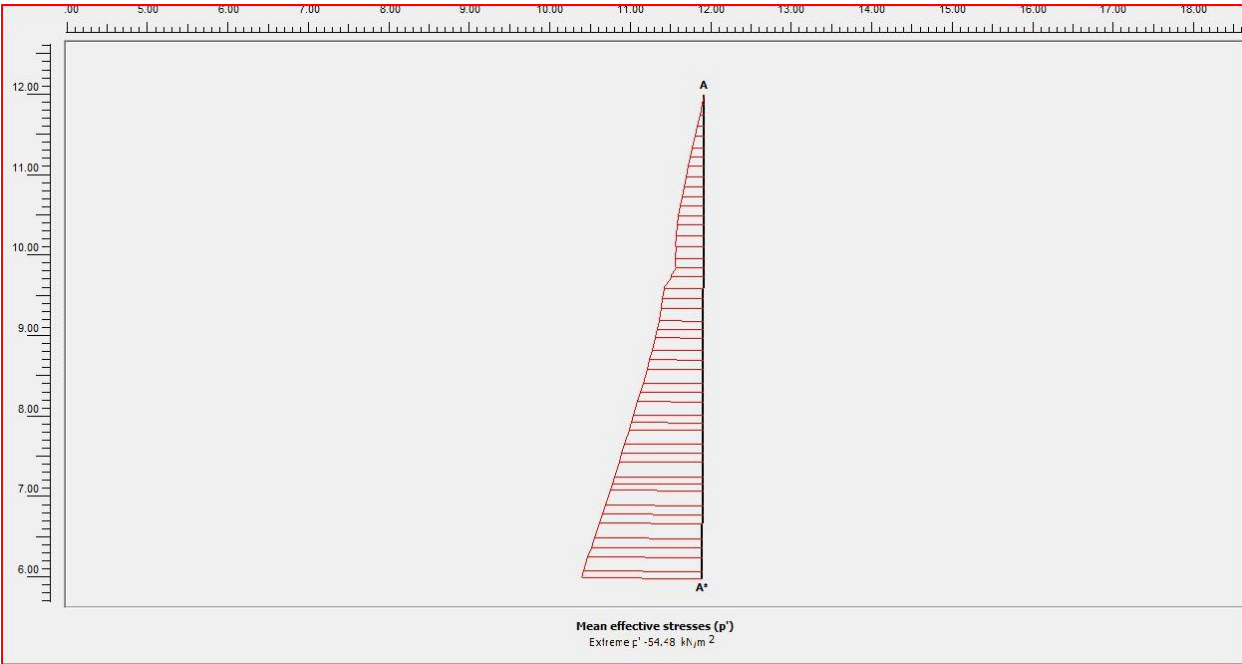


Fig 3.29 Distribution of effective stress on retaining wall by slag

Table 3.1 Extreme earth pressure for different materials

Material	Sand	Red mud	Fly ash	Crusher dust	Slag
Max. Earth Pressure (kPa)	36.31	58.50	27.36	53.70	54.48

In the above study it can be seen that the active earth pressure acting on retaining wall is found to be maximum in case of red mud when used as backfill followed by slag, crusher dust, sand and fly ash which is represented in the Table 3.1.

3.3 INCLINED RETAINING WALL

The value of active earth pressure has direct relation to the angle of wall. It means by reduction of inclination angle from vertical state the value of active earth pressure will decrease. However only a few analytical solutions has been reported in design codes or published researches for calculating the active earth pressure which is usually smaller in inclined walls than vertical walls. Ghanbari and Ahmadabadi (2009) have proposed several formulae to calculate the active earth pressure by considering limit equilibrium method. Necessary parameters are extracted assuming the pseudo static seismic coefficient to be valid in earthquake conditions.

Using analytical relations based on equilibrium of forces and moments in a failure wedge, characteristics of active earth pressure in static and pseudo-static conditions for inclined walls is calculated using 'C' coding. In our work we have developed a 'C' program to calculate the active earth pressure.

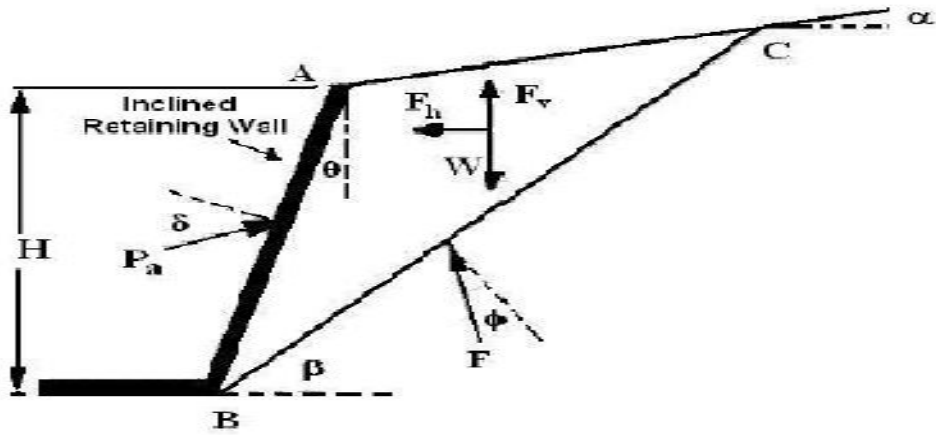


Fig 3.29 Schematic diagram of inclined retaining wall

where, β = angle of failure wedge

θ = angle of inclination of the wall

α = angle of the back fill

P_{ae} = active earth pressure

Figure 3.30 shows the variation of active earth pressure on the retaining wall for different angle of inclination of the wall for different materials. It can be seen that earth pressure reduces with increase in angle of retaining wall. It was also observed that maximum active earth pressure was observed for red mud, followed by crusher dust, fly ash, slag and sand. High earth pressure value of red mud is due to its high density value and comparative low ϕ value. Similarly the fly ash has considerably less earth pressure value due to its low density value.

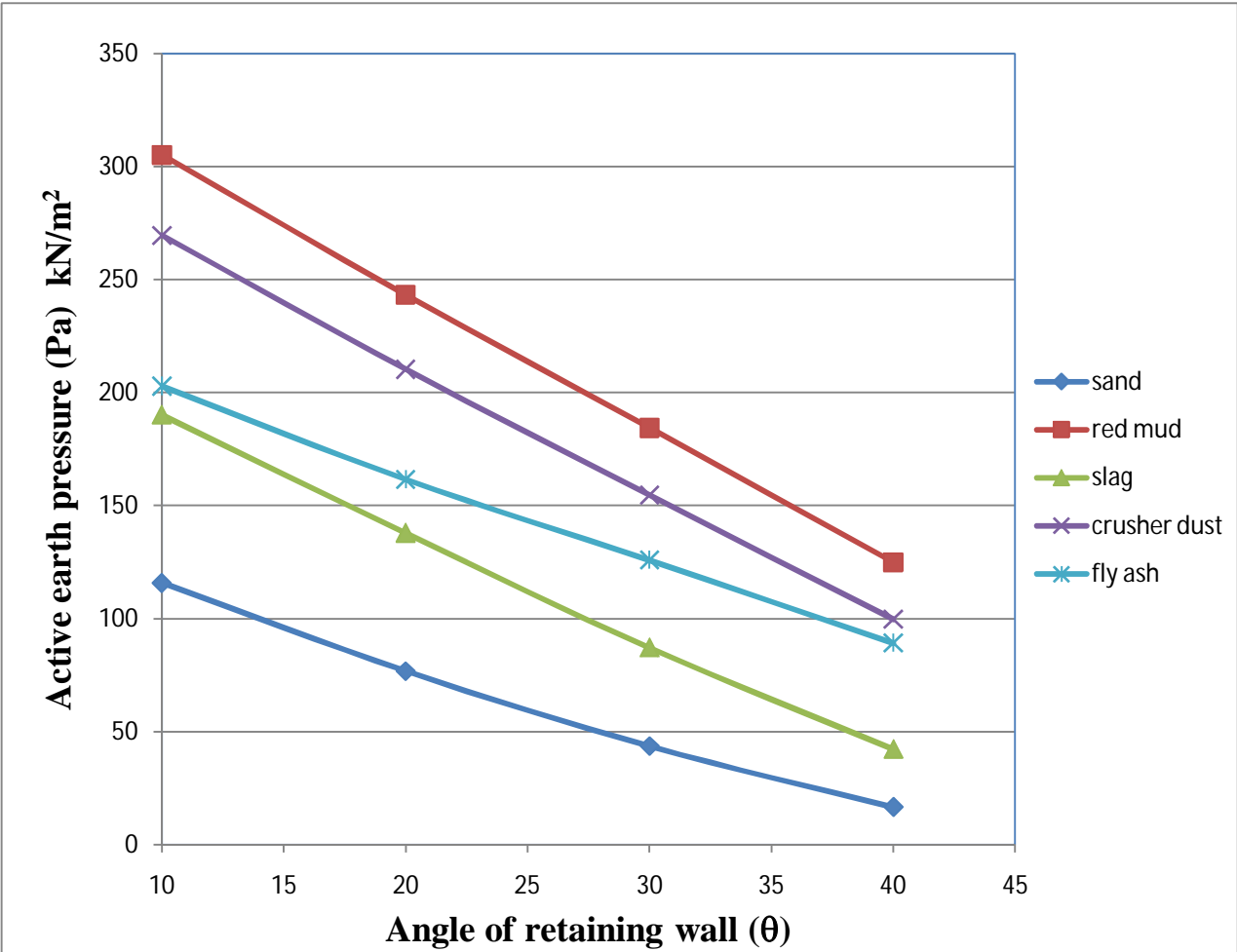


Fig 3.30 Active earth pressure against angle of inclination of wall for different materials

CHAPTER-4

RELIABILITY ANALYSIS OF SHALLOW FOUNDATIONS

4.1 RELIABILITY

Uncertainty and Reliability have a long background in geotechnical engineering. Even before discovery of a particular distinct field of geotechnical engineering, engineers who were involved with rocks, soils and geological phenomena knew that they were involved in an uncertain venture and have to provide some solution to these difficult developments. It has also been found out that one of Terzaghi's early papers (Terzaghi 1929) emphasizes the importance of geologic details – features that differ from expected conditions. He recommended that designers should “assume the most unfavourable possibilities.”

Reliability is the ability of a system to perform satisfactorily without reaching the limit state for a specified period of time (design period) or it is also defined as the probabilistic measure of the assurance of the performance of a system.

The traditional design methodologies mostly depend on global factor of safety approach (working stress design) or partial factor approach (limit state design), whereby the variability in the design parameters are considered by a unique factor of safety/partial factors. But there is variability of 5-240% in case of soil properties (Becker 1996). Thus a single factor of safety to load or resistance or partial safety factors considered for both are not sufficient to take into account the whole uncertainty associated to the various design parameters in geotechnical engineering problem. In geotechnical engineering problems source of uncertainties are mainly due to the inherent spatial variability of soil properties, uncertainties in loading conditions, presence of geologic anomaly, uncertainty associated with selection of an appropriate analytical model, testing and measurements errors, human errors.

Risk of failure of any geotechnical system can be reduced by considering the variability of the parameters contributing to the performance of the system. This can be achieved by identifying the most frequent cause of failure and resorting to *reliability analysis*.

4.2 RELIABILITY ANALYSIS

For computational purpose reliability can be taken as the probability of survival and is equal to one minus the probability of failure.

Let the resistance of a simple one element of structure be R and the load on the structure be L. The structure is said to fail when R is less than L and its probability of failure (p_f) is given as

$$p_f = P[R \leq L] = P[(R - L) \leq 0] \tag{4.1}$$

The performance function can be expressed as as, $Z = (\text{margin of safety}) = (R - L) = g(R, L) = g(X_1, X_2, X_3, \dots, X_n)$. When this performance function is equal to zero, i.e., $g(X_1, X_2, X_3, \dots, X_n) = 0$, it is called the *failure surface equation* or *the limit state equation* which defines a hyper surface in the basic variable space and defines the unsafe region. This failure surface may be linear or non linear.

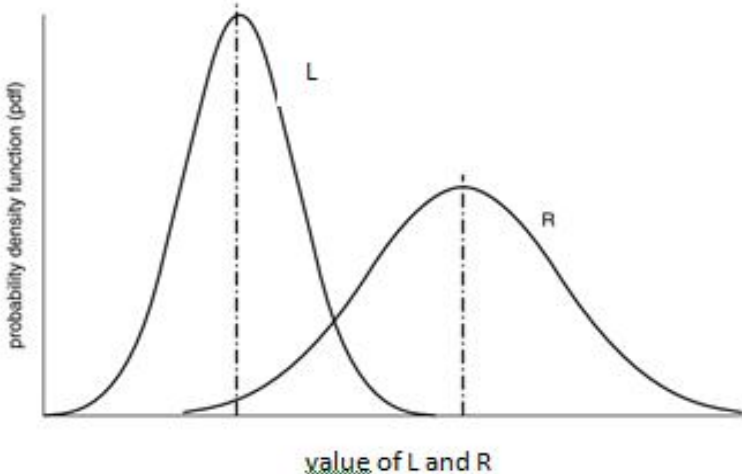


Fig. 4.1 The overlapped area as probability of failure of random variable R and L

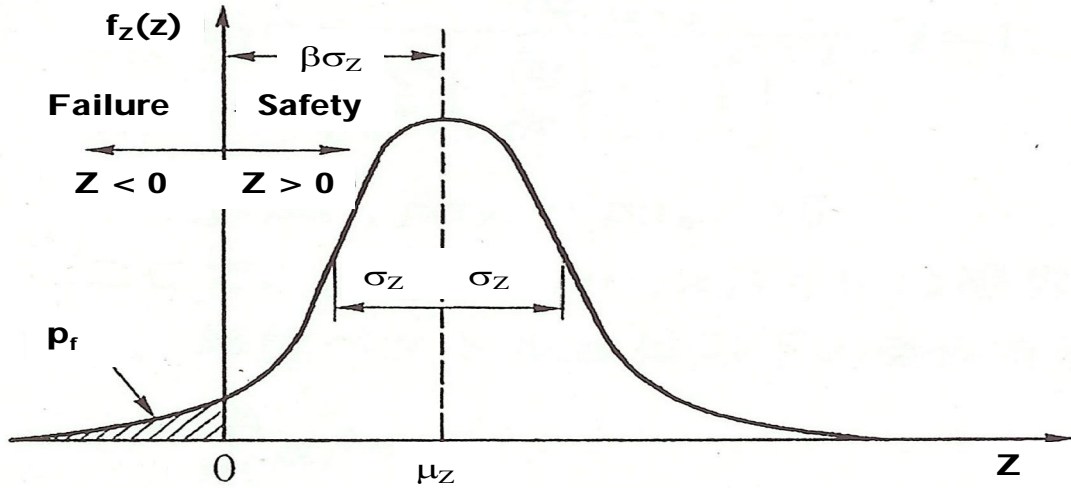


Fig. 4.2 Distribution of safety margin, $Z = R-L$ (Melchers 2002)

The failure function Z follows *normal* distribution, if R and L both follows normal distribution with μ_R , μ_L and σ_R , σ_L are the means and standard deviations respectively. The reliability of the system can be quantified by reliability index, β , was first defined by Cornell

$$\beta = \frac{\mu_z}{\sigma_z} \quad (4.2)$$

where μ_z and σ_z are the mean and standard deviation of the random variable Z . If R and L normal and uncorrelated then β can be expressed as

$$\beta = \frac{\mu_R - \mu_L}{\sqrt{\sigma_R^2 + \sigma_L^2}} \quad (4.3)$$

$$p_f = P(Z < 0) \quad (4.4)$$

$$p_f = 1 - \Phi \left[\frac{(\mu_R - \mu_L)}{\sqrt{\sigma_R^2 + \sigma_L^2}} \right] \quad (4.5)$$

$$p_f = 1 - \Phi [\beta] \quad (4.6)$$

Φ is the Cumulative Density Function of standard normal variable. **Table 4.1** shows the relationship between β and (p_f) for different level of performance of the system.

Table 4.1 The expected levels of Performance in terms p_f and corresponding β (U.S. Army Corps of Engineers 1999)

Expected performance	Reliability index(β)	Probability of failure (p_f)
High	5.0	0.0000003
Good	4.0	0.00003
Above average	3.0	0.001
Below average	2.5	0.006
Poor	2.0	0.023
Unsatisfactory	1.5	0.07
Hazardous	1.0	0.16

4.3 METHODS OF RELIABILITY

Methods of reliability analysis can be classified on the basis of types of calculations performed and approximations made.

I. **Level-3 methods:** These are most advanced methods known as full distribution approach.

They can be characterized as probabilistic methods of analysis as based on the knowledge of joint probability distribution function of all basic variables. Use of these methods involves practical problems as there is always scarcity of sufficient data of different variables to define the joint PDF. It is also extremely difficult to evaluate the multidimensional integration.

II. **Level-2 methods:** These methods are based on some analytical approximation to solve the complicated integral as followed in the Level-3 methods. Again under this group methods are classified as

- i. First order reliability methods (FORM)
- ii. Second order reliability method (SORM)

The probability of failure as determined from the Level -2 methods can be verified by using simulation techniques such as

- i. Monte Carlo simulation method (MCS)
- ii. Importance sampling method (ISM)
- iii. Adaptive sampling method (ASM)

First Order Reliability Method:

The shortcoming of the First Order Second Moment approach is that the results purely depend on the values of variables used at which the partial derivatives are calculated, as it is difficult to evaluate partial derivatives directly. The difficulty was resolved by the proposed theory by Hasofer and Lind (1974) in which the derivatives are evaluated at the critical point on the failure surface. The critical point (design point) can be obtained by iterations, which tends to converge rapidly. The variables are normalized by dividing by their respective standard deviations, the distance between the failure points and the point defined by the normalized means is called the reliability index β .

4.4 CALCULATION OF RELIABILITY INDEX

The Solver Add-in in Microsoft Office Excel was used to study the Reliability analysis for the combination of soils. The soil property values calculated in **Chapter-2** were used to calculate the bearing capacity of industrial wastes. The bearing capacity was calculated by using the Terzaghi's equation given in equation **1.1a** and **1.1b**. The results are shown in **Figure 4.3**.

	A	B	C	D	E	F	G	H	I	J
				HOMOGENEOUS SOIL						
		c	ϕ	γ		Nq	$N\gamma$	Nc		qu
		kN/m ²	degrees	kN/m ³						kN/m ²
5	sand	0.31	38.52	15.10		52.45	85.09	64.63		2888.81
7	red mud	13.87	26.00	21.40		11.85	12.54	22.25		1084.36
8	slag	0.94	34.77	21.00		32.36	46.32	45.17		2374.27
9	crusher dust	0.31	27.70	20.50		14.24	16.01	25.23		919.94
0	fly ash	19.68	24.37	12.90		9.98	9.95	19.83		776.00
1										
2										
3										

Fig. 4.3 Bearing capacity of individual industrial waste

Combinations of industrial waste were used to study the Reliability analysis and calculate the value of reliability index. In the present study slag, crusher dust and fly ash were combined together to calculate the reliability index.

Using Terzaghi's equation (1.1a and 1.1b) ultimate bearing capacity of industrial waste was calculated and is shown in the spreadsheet (Figure 4.4).

	A	B	C	D	E	F	G	H	I	J	K
13					COMBINATION						
14											
15						c_cov	φ_cov	Υ_cov	Nq	NY	Nc
16	slag	0.94	34.77	21.00		0.25	0.15	0.07	16.35	19.19	27.75
17	crusher dust	0.31	27.70	20.50							
18	fly ash	19.68	24.37	12.90		c_+	φ_+	Υ_+	Nq_+	NY_+	Nc_+
19						9.85	36.11	20.23	38.29	57.32	51.11
20		c_mean	φ_mean	Υ_mean							
21		6.98	28.95	18.13		c_-	φ_-	Υ_-	Nq_-	NY_-	Nc_-
22						4.10	21.78	16.04	7.65	6.91	16.64
23											
24			c	φ	Υ		qu				
25	0 0 0		9.85	36.11	20.23		3212.20				
26	0 0 1		9.85	36.11	16.04		2651.32			0 represents +ve	
27	0 1 0		9.85	21.78	20.23		613.36			1 represents -ve	
28	0 1 1		9.85	21.78	16.04		520.31				
29	1 0 0		4.10	36.11	20.23		2918.00				
30	1 0 1		4.10	36.11	16.04		2357.12				
31	1 1 0		4.10	21.78	20.23		517.57				
32	1 1 1		4.10	21.78	16.04		424.52				
33											

Fig. 4.4 Bearing capacity of combined industrial waste (using Terzaghi's equation)

During the study several equations were considered and results were calculated. The most appropriate equation (4.7) leaving minimum residue was then used.

$$q_u = C_1(c^{C_2}) + C_3(\phi^{C_4}) + C_5(\gamma^{C_6}) \quad (4.7)$$

where $C_1, C_2, C_3, C_4, C_5, C_6$ are constants.

With the help of Microsoft Excel Solver all the constants value were determined and then according to the equation 4.7 bearing capacity was calculated, which is shown in Figure 4.5.

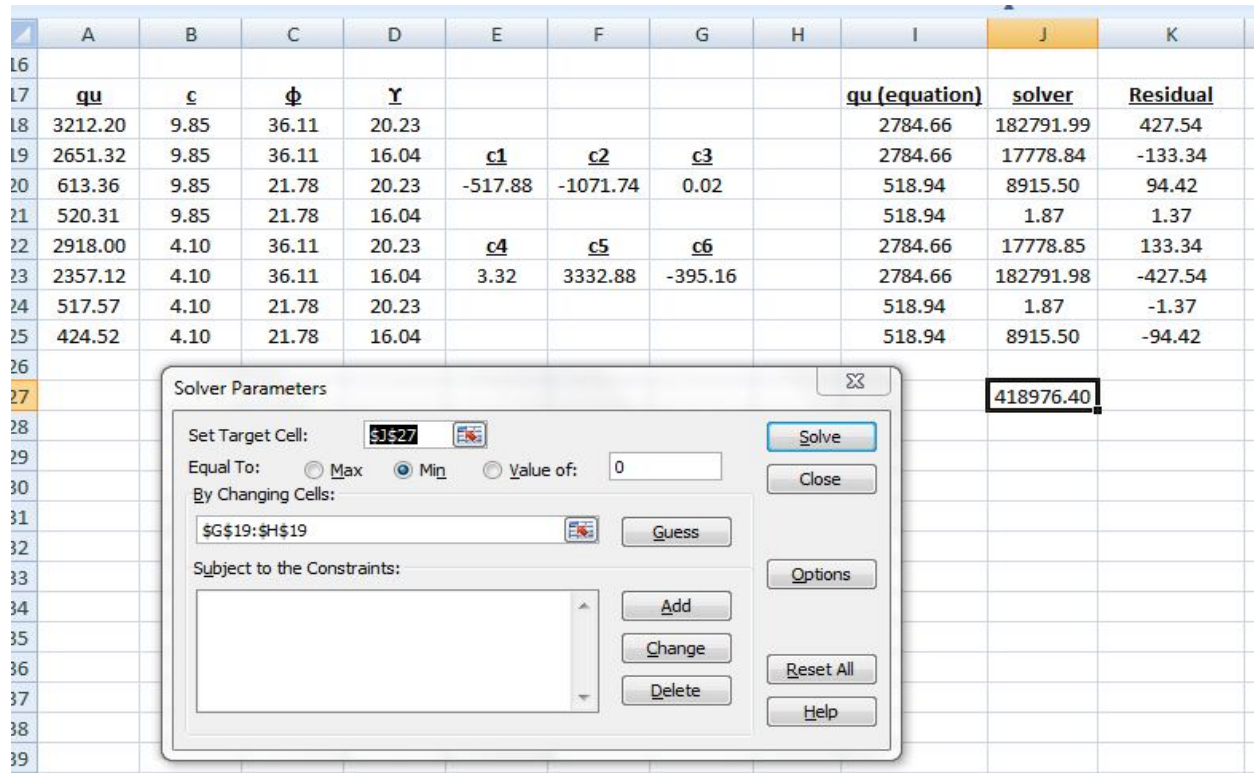


Fig. 4.5 Bearing capacity of combined industrial waste (using equation 4.11)

RELIABILITY INDEX

$$\beta = \sqrt{XX^T} \quad (4.8)$$

$$X = \begin{Bmatrix} \frac{c - \mu_c}{\sigma_c} \\ \frac{\phi - \mu_\phi}{\sigma_\phi} \\ \frac{\gamma - \mu_\gamma}{\sigma_\gamma} \end{Bmatrix} \quad (4.9)$$

where μ = mean

σ = standard deviation

β = reliability index

$$\text{Performance function: } g(x) = q_u - q \quad (4.10)$$

where q_u is taken from equation 4.7 and q is taken as load acting on footing i.e 250 kN/m² in the present study.

Figure 4.6 gives the Reliability index and also the design points satisfying the given constraint condition.

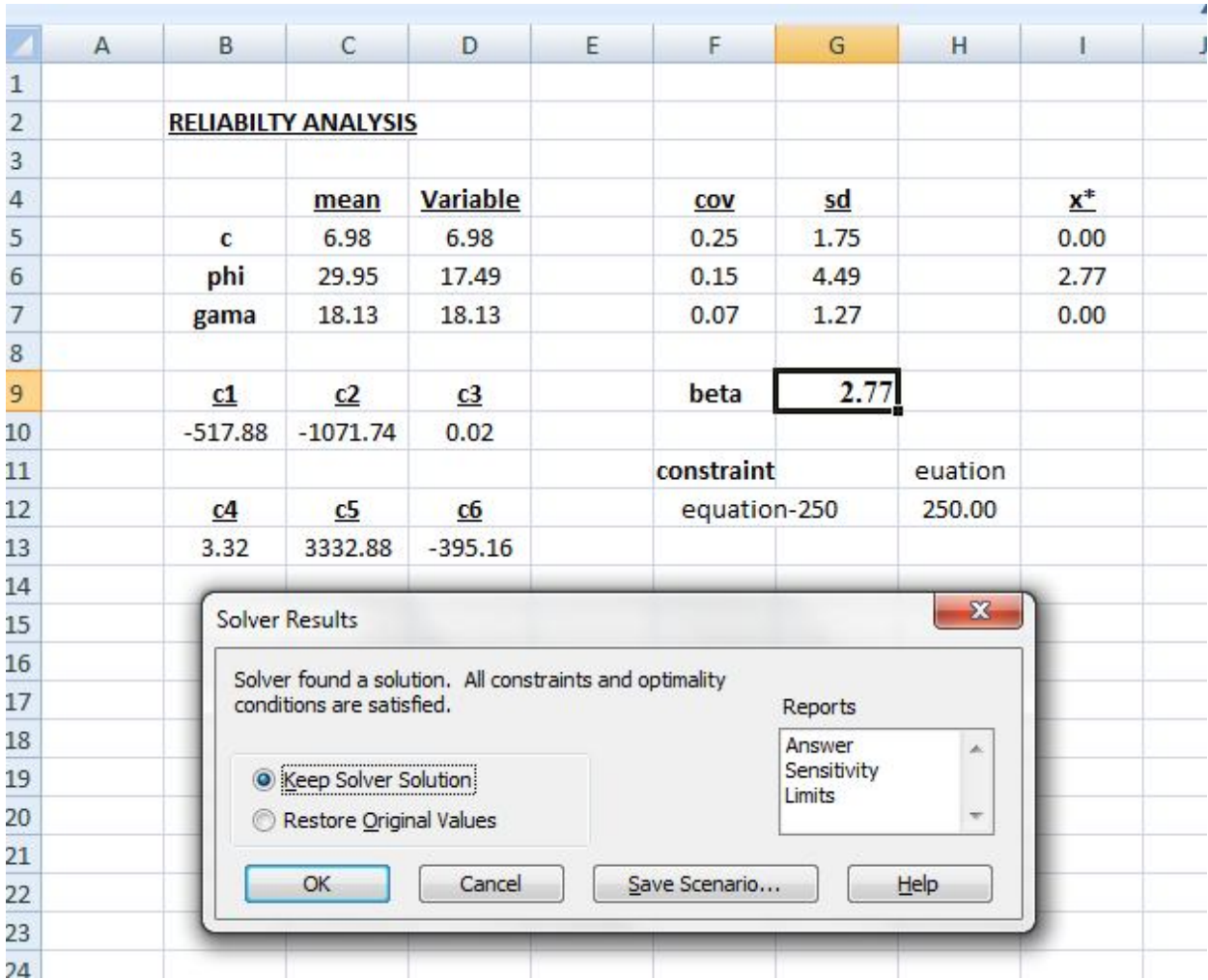


Fig. 4.6 Reliability Index for the combination of sample

From the Microsoft Excel Solver we get the Reliability Index value as 2.77 which show that the expected performance for the shallow foundation under the applied load would be average and the failure probability comes to around 0.3%.

CHAPTER-5
CONCLUSION AND SCOPE FOR
FUTURE WORK

5.1 CONCLUSIONS

Rapid industrialization has resulted in accumulation of huge quantities of industrial waste. Disposal of industrial waste is covering vast track of valuable land and also polluting environment. Remedy lies in effective utilization of these wastes in large quantities. In this study an attempt has been made to evaluate the properties of industrial wastes like fly ash, red mud, crusher dust, blast furnace slag to use as foundation bed and backfill in retaining structures. An attempt also has been made to use reliability analysis for foundation on industrial waste based on the properties of the wastes as per laboratory investigations. Based on the laboratory investigation and finite element/ limit equilibrium analysis made thereof following conclusions can be made.

- (i) The industrial wastes are found to be potential geotechnical engineering materials.
- (ii) The specific gravity of red mud is found to be 3.06 which is maximum and fly ash was found to have minimum specific gravity of 1.98. However, the red mud is found to have the maximum dry density values and fly ash is found to have lowest maximum dry density.
- (iii) The angle of internal friction in case of natural sand is found to be more compared to all other industrial wastes.
- (iv) The bearing capacity found to decrease with increase in slope angle and also decreases with increase in seismic forces.
- (v) For the inclined retaining wall, maximum active earth pressure was observed for red mud, followed by crusher dust, fly ash, slag and sand. High earth pressure value of red mud may be due to its high density value and comparative low ϕ value. Similarly the fly ash has considerably less earth pressure value due to its low density value.

- (vi) Based on reliability analysis of a typical footing on a hypothetical soil with properties lying between the properties of industrial wastes, the reliability index was found to be 2.77, which corresponds to average performances and probability of failure as 0.3%. The corresponding SBC is found to be 250 kN/m².

5.2 SCOPE OF FUTURE STUDIES

Based on the above study it was observed that many further studies are required in this direction for more effective utilization of these wastes. Some of the following problems are recognized for further studies.

- (i) In-situ tests on the dumped industrial wastes
- (ii) Long term strength characterization of the industrial wastes
- (iii) Reliability analysis of different geotechnical structures using industrial wastes

APPENDIX

/* The code below gives the Active Earth Pressure on the Retaining Wall */

```
#include "stdio.h"
```

```
#include "math.h"
```

```
main()
```

```
{
```

```
float A,B,C,alpha,beta,teta,delta,phi,x,y,z,
```

```
alpha_r,teta_r,phi_r,beta_r,delta_r,kh,kv,H,m,n,gamma,Pae;
```

/*Entering the property of soil */

```
printf("\nenter the value of alpha : ");
```

```
scanf("%f",&alpha);
```

```
printf("\nenter the value of gamma : ");
```

```
scanf("%f",&gamma);
```

```
printf("\nenter the value of phi : ");
```

```
scanf("%f",&phi);
```

```
printf("\nenter the value of teta : ");
```

```
scanf("%f",&teta);
```

/*Defining the retaining wall dimensions*/

```
H = 10;
```

```
kh = .01;
```

```
kv = .01;
```

```
delta = 2*phi/3;
```

```

alpha_r = alpha*3.14/180;
delta_r = delta*3.14/180;
phi_r = phi*3.14/180;
teta_r = teta*3.14/180;
A = tan(phi_r-alpha_r);
B = tan(phi_r+teta_r);
C = tan(teta_r-delta_r);
printf("\n");

z = -(C*kh)+(A*B);
y = C+(A*B*C)-B-(B*C)*kh;
x = sqrt((1+C*kh)*(A-kh)*(1+A*B)*(B-C));

beta = phi+(180/3.14)*atan((z-x)/y);
printf("beta=%f",beta);
printf("\n");

beta_r = beta*(3.14/180);
n = (kh/tan(beta_r-phi_r))/(1-kv);
m = ((cos(teta_r+alpha_r))*(cos(teta_r+beta_r))*(sin(beta_r-phi_r)))/((cos(teta_r))*(cos(teta_r))*(sin(beta_r-alpha_r))*(cos(teta_r-delta_r-phi_r+beta_r)));

/*Calculation of active earth pressure*/
Pae = 0.5*gamma*H*H*m*n;
printf("\n");
printf("Pae = %f ",Pae);
}

```

REFERENCES

REFERENCES

- [1] Christian, J. T. (2004). “**Geotechnical Engineering Reliability: How Well Do We Know What We Are Doing?**”, Journal of Geotechnical and Geoenvironmental Engineering, ACSE Vol. 130, No. 10.
- [2] Choudhury, D., and Subba Rao, K. S. (2005). “**Seismic bearing capacity of shallow strip footings.**” *J. Manuf. Syst.*, 24_1_, 117–127.
- [3] Das, B. M. (1999). **Principles of foundation engineering**, 4th Ed., Publishing Workflow System, Pacific Grove, Calif
- [4] Ghanbari, A., and Ahmadabadi, M., “**Active Earth Pressure on Inclined Retaining Walls in Static and Pseudo-Static Conditions**”. April 2010.
- [5] **IS 1904 : 1986** Code of practice for design and construction of foundations in soils: general requirements
- [6] **IS 2720 : Part 3 : Sec 1 : 1980** Methods of test for soils: Part 3 Determination of specific gravity Section 1 fine grained soils
- [7] **IS 2720 : Part VII : 1980** Methods of Test for Soils - Part VII : Determination of Water Content-Dry Density Relation Using Light Compaction
- [8] **IS 2720 : Part 8 : 1983** Methods of Test for Soils - Part 8 : Determination of Water Content-Dry Density Relation Using Heavy Compaction
- [9] **IS 2720 : Part 13 : 1986** Methods of Test for Soils - Part 13 : Direct Shear Test
- [10] **IS 6403 : 1981** Code of practice for determination of bearing capacity of shallow foundations

- [11] **Kumar, J. & Mohan Rao, V. B. K.** (2003). *Géotechnique* 53, No. 3, 347–361.
347. **Seismic bearing capacity of foundations on slopes**
- [12] Meyerhof, G. G. (1957). **The ultimate bearing capacity of foundations on slopes.**
Proc. 4th Int. Conf. Soil Mech. Found. Engng, London 1, 384–386.
- [13] Meyerhof, G. G. (1963). **Some recent research on the bearing capacity of foundations.** *Can. Geotech. J.* 1, No. 1, 16–26.
- [14] Richards, R., Elms, D. G. & Budhu, M. (1993). **Seismic bearing capacity and settlement of foundations.** *J. Geotech. Engng Div., ASCE* 119, No. 4, 662–674.
- [15] Sivakumar Babu, G. L., and Basha B. M., **“Optimum Design of Cantilever Retaining Walls Using Target Reliability Approach”**. August 2008.